Tampereen teknillinen korkeakoulu
Julkaisuja 375

Tampere University of Technology
Publications 375

Ridha Hamila

Synchronization and Multipath Delay Estimation Algorithms for Digital Receivers

Tampere 2002

Tampereen teknillinen korkeakoulu
Julkaisuja 375

Tampere University of Technology
Publications 375

Ridha Hamila

Synchronization and Multipath Delay Estimation Algorithms for Digital Receivers

Thesis for the degree of Doctor of Technology to be presented with due permission for public examination and criticism in Tietotalo Building, Auditorium TB109, at Tampere University of Technology, on the 19th of June 2002, at 12 o'clock noon.

Tampere 2002

ISBN 952-15-0838-8 (printed)
ISBN 952-15-1836-7 (PDF)
ISSN 0356-4940

TTKK- PAINO, Tampere 2002

ABSTRACT

This thesis considers the development of synchronization and signal processing techniques for digital communication receivers, which is greatly influenced by the digital revolution of electronic systems. Eventhough synchronization concepts are well studied and established in the literature, there is always a need for new algorithms depending on new system requirements and new trends in receiver architecture design. The new trend of using digital receivers where the sampling of the baseband signal is performed by a free running oscillator reduces the analog components by performing most of the functions digitally, which increases the flexibility, configurability, and integrability of the receiver. Also, this new design approach contributes greatly to the software radio (SWR) concept which is the natural progression of digital radio receivers towards multimode, multistandard terminals where the radio functionalities are defined by software.

The first part of this research work introduces a new technique for jointly estimating the symbol timing and carrier phase of digital receivers with non-synchronized sampling clock for both data-aided and non-data-aided systems using a block-based feed-forward architecture. This technique is a practical, rapidly converging, fully digitally implemented synchronization concept based on a low-order polynomial approximation of the likelihood functions using the Farrow-based interpolator. A review of maximum likelihood theory, which is the basis for coherent theory of synchronization, defines first the criteria and general framework for developing near-optimum synchronization schemes for digital communication systems. Then, efficient Farrow-based polynomial approximations of the typical likelihood functions are derived for systematic symbol timing, carrier phase and fine acquisition frequency synchronization algorithms.

Another important receiver functionality closely related to synchronization is propagation delay estimation which is the basis of positioning technologies. Mobile phone positioning is becoming unavoidable after the mandate imposed by communications regulatory bodies on emergency call positioning. The second part of this thesis reviews and develops new techniques with subchip resolution capabilities for estimating closely-spaced multipath delays in spread-spectrum CDMA systems. Generally, multipath delays caused by distant reflectors have relatively large delay spread, with more than one chip interval between different paths, that can be resolved using conventional delay-locked-loop techniques. However, shorter excess path delays result in overlapped fading multipath components that introduce significant errors to the line-of-sight path delay and gain estimation. Overlapping fading multipath components are considered as one of the major sources of error that have strong impact on high precision mobile positioning solutions, as well as, on mobile applications of dedicated systems like the Global Positioning System (GPS). An overview of the most promising geolocation positioning techniques for wireless systems that are being standardized is first provided with a survey of fundamental concepts and major problems in positioning. Then, the characteristics of different channel models and conventional multipath delay estimation techniques based on maximum likelihood theory are also discussed. Two new techniques with subchip resolution capabilities are proposed for estimating closely-spaced overlapped multipath components. These techniques are intended to improve the accuracy of location estimates by estimating correctly the delay of the line-of-sight path.

Preface

Research work for this thesis has been carried out during the years 1997-2002 in the research project "Advanced Transceiver Architectures and Implementations for Wireless Communications" at the Institute of Communications Engineering (formerly Telecommunications Laboratory) of Tampere University of Technology, Finland. This thesis was financially supported by the Academy of Finland and Tampere Graduate School of Information Science and Engineering (TISE), which are gratefully acknowledged.

First, I would like to express my sincere and deep gratitude to my supervisor Professor Markku Renfors for his invaluable guidance, continuous support, and infinite tolerance during the course of this work.

I would like to thank Associate Professor Peter Händel from the Department of Signals, Sensors and Systems, Royal Institute of Technology, Stockholm, and Professor Timo Laakso from the Signal Processing Laboratory, Helsinki University of Technology, for reviewing my thesis, and for their constructive feedback and comments on the manuscript.

Special thanks are due to Professor Jaakko Astola my former M.Sc. advisor, to Professor Moncef Gabbouj for his encouragement as well as for his kind advice, to Professor Tapio Saramäki for creating an enthusiastic work atmosphere, to professor Jarmo Harju, Dr. Pertti Koivisto coordinator of TISE, to Dr. Jari Syrjärinne, to Professor fred harris for giving me the opportunity to visit San Diego State University, California, and to Professor James F. Kaiser for sharing with me Teager energy concept and scientific experience.

I am indebted to all my colleagues and friends at the Institute of Communications Engineering for the pleasant work environment and for the help I have received during my work. I owe special thanks to Dr. Jussi Vesma and M.Sc. Simona Lohan for their cooperation, suggestions, and for the fruitful technical discussions, as well as, to Dr. Juha Yli-Kaakinen for the LaTeX help. In particular special thanks are due to Tarja Erälaukko, Sari Kinnari and Elina Orava.

Special thanks to all my friends in Finland for their support and care. I'm very obliged to Mohamed Maala, family Gabbouj, Faouzi Alaya Cheick, Saara Maala, Vesma family, Paula Linna, Ali Hazmi, family Hammouda, Monaem Lakhzouri, Mejdi Trimeche, Mika Nieminen, Sari Luhtala, Asheesh family, Abdo family, and to the small Tunisian community in Tampere.

Most of all I wish to express my deepest gratitude to Satu Lassila, my mother Fatma, my brothers and sisters for their love, endless support, encouragement, and understanding all these years.

Finally, I would like to dedicate this thesis to the memory of my father Salem who did not have the chance to see the outcome of this work, God bless him.

RIDHA HAMILA

Tampere, May 31, 2002

Contents

Preface **iii**

List of Publications **ix**

List of Supplementary Publications **xi**

List of Symbols and Acronyms **xiii**

1 Introduction **1**

2 Polynomial-Based ML Technique for Synchronization in Digital Receivers **5**
2.1 Introduction 5
2.2 Synchronization and Timing Recovery Techniques 6
2.3 Maximum Likelihood Estimation 6
2.3.1 ML Principle for Optimum Receivers 6
2.3.2 Likelihood Function for Systematic Synchronization Algorithms . . 9
2.3.3 Data-Aided Estimation 11
2.3.4 Non-Data-Aided Estimation 12
2.4 Timing Adjustment Using Polynomial Interpolation 13
2.4.1 Receiver with Non-Synchronized Sampling 13
2.4.2 The Farrow Structure 13
2.5 Polynomial Approximation for the Log-Likelihood Function 15
2.5.1 Data-Aided Estimator 15
2.5.2 Non-Data-Aided Estimator 17
2.6 Summary of Simulation Results 18

3 Multipath Delay Estimation for Accurate Positioning **21**
3.1 Introduction 21
3.2 Techniques for Personal Positioning: Principles and Problems 21

3.3 Fundamentals of GPS 24
3.3.1 Satellite Signals 25
3.3.2 Signal Characteristics 26
3.4 Multipath Delay Estimation Techniques 27
3.4.1 Channel Models 27
3.4.2 Conventional ML Based Approaches 29
3.4.3 Multipath Delay Estimation Using Peak Tracking with Pulse Subtraction 31
3.4.4 Multipath Delay Estimation Based on Teager-Kaiser Operator 33

4 Summary of Publications **37**
4.1 Receiver Synchronization Studies 37
4.2 Multipath Delay Estimation Studies 38
4.3 Author's Contribution to the Publications 39

5 Conclusions **41**

References **43**

Publications **47**

List of Figures

2.1 Timing recovery methods. 7

2.2 Degradation of symbol error probability due to different timing errors, $\Delta\tau$, using QPSK modulation. 8

2.3 Degradation of symbol error probability due to different phase errors, $\Delta\phi$, using QPSK modulation. 8

2.4 Digital receiver with non-synchronized sampling. 11

2.5 Illustrative example of a typical log-likelihood function for $\tau_0 = 0.52T$ and $\theta_0 = 0$, as well as its first order derivative. 11

2.6 The Farrow structure for polynomial-based interpolation filter. 14

2.7 Example of the input and output samples for the Farrow structure. Here the over-sampling ratio is $\beta = T/T_s = 2$. 14

2.8 DA symbol timing and carrier phase synchronization scheme. 17

2.9 NDA symbol timing recovery scheme. 18

2.10 NDA carrier phase estimation scheme for M-PSK modulations. 19

3.1 Principles of E-OTD and A-GPS methods in cellular network. 23

3.2 GPS signal structure. 25

3.3 GPS signal spectrum (positive side). 26

3.4 User received minimum power levels with respect to the user elevation angle and signal structure. 27

3.5 Non-coherent DLL S-curve for a multipath channel. 31

3.6 Effect of multipath propagation on the S-curve of a non-coherent DLL using different discriminator values Δ and two paths channel. 32

List of Publications

[P1] R. Hamila, J. Vesma, T. Saramäki and M. Renfors, "Discrete-Time Simulation of Continuous-Time Systems Using Generalized Interpolation Techniques," *in Proc. 1997 the Summer Computer Simulation Conference,* SCSC'97, Arlington, Virginia, USA, July 1997, pp. 914–919.

[P2] R. Hamila, J. Vesma, H. Vuolle, and M. Renfors, "Joint Estimation of Carrier Phase and Symbol Timing Using Polynomial-Based Maximum Likelihood Technique," *in Proc IEEE 1998 International Conference on Universal Personal Communications,* ICUPC'98, Florence, Italy, October 1998, pp. 369–373.

[P3] R. Hamila, J. Vesma, H. Vuolle, and M. Renfors, "NDA Maximum Likelihood Approach for Timing and Phase Adjustment by Polynomial-Based Interpolation," *in Proc. 6th IEEE International Workshop on Intelligent Signal Processing and Communication Systems,* ISPACS'98, Melbourne, Australia, Nov. 1998, pp. 248–252.

[P4] R. Hamila, J. Vesma, H. Vuolle, and M. Renfors, "Effect of Frequency Offset on Carrier Phase and Symbol Timing Recovery in Digital Receivers," *in Proc. 1998 URSI International Symposium on Signals, Systems, and Electronics,* ISSSE'98, Pisa, Italy, September 1998, pp. 247–252.

[P5] R. Hamila, M. Renfors, "New Maximum Likelihood Based Frequency Estimator for Digital Receivers," *in Proc. IEEE Wireless Communications and Networking Conference,* WCNC´99, New Orleans, USA, Sept. 1999, pp. 206–210.

[P6] R. Hamila, S. Lohan, and M. Renfors, "Effect of Correlation Estimation on Multipath Delay Estimation Techniques in DS-CDMA Systems," *in Proc. of 4th International Symposium on Wireless Personal Multimedia Communications,* WPMC'01, Aalborg, Denmark, September 2001, pp. 331–335.

[P7] R. Hamila, S. Lohan, and M. Renfors, "Novel Technique for Closely-Spaced Multipath Delay Estimation in DS-CDMA Systems," *Submitted to Signal Processing,* (EURASIP).

[P8] S. Lohan, R. Hamila, and M. Renfors, "Performance Analysis of an Efficient Multipath Delay Estimation Approach in a CDMA Multiuser Environment," *in Proc. of 12th IEEE International Symposium on Personal, Indoor and Mobile Radio Communications,* PIMRC´01, San Diego, California, USA, Sept. 2001, pp. 6–10.

List of Supplementary Publications

[S1] R. Hamila, J. Vesma and M. Renfors, "Polynomial-Based Maximum Likelihood Technique for Synchronization in Digital Receivers," *to be published in the IEEE Transactions on Circuit and Systems II: Analog and Digital Signal Processing.*

[S2] J. Vesma , R. Hamila, T. Saramäki and M. Renfors, "Design of Polynomial Interpolation Filters Based on Taylor Series," *in the European Signal Processing Conference,* Rhodes, Greece, September 1998, pp. 283–286.

[S3] R. Hamila, J. Astola, F. Alaya Cheikh, M. Gabbouj, and M. Renfors, "Teager Energy and the Ambiguity Function," *IEEE Transactions on Signal Processing*, Vol. 47, No. 1, pp. 260–262, January 1999.

[S4] R. Hamila, F. Alaya Cheikh, J. Vesma, J. Astola, and M. Gabbouj, "Relationship between Wigner-Distribution and the Teager Energy," *in Proc. European Signal Processing Conference,* Rhodes, Greece, September 1998, pp. 1857–1860

[S5] R. Hamila, M. Renfors, G. Gunnarsson, M. Alanen, "Data Processing for Mobile Phone Positioning," *in Proc. Vehicular Technology Conference,* Amsterdam, Netherlands, Sept. 1999, pp. 446–449.

[S6] R. Hamila, S. Lohan, and M. Renfors, "Novel Technique for Multipath Delay Estimation in GPS receivers," *in Proc. IEEE International Conference on Third Generation Wireless and Beyond,* San Francisco, USA, May 2001, pp. 993–998.

[S7] S. Lohan, R. Hamila, and M. Renfors, "Cramer Rao Bound for Multipath Time Delays in a DS-CDMA System," *in Proc. of 4th International Symposium on Wireless Personal Multimedia Communications,* Aalborg, Denmark, September 2001, pp. 1043–1046.

[S8] R. Hamila, S. Lohan and M. Renfors, "Subchip Multipath Delay Estimation for Downlink WCDMA System Based on Teager Operator," *Submitted to IEEE Communications Letters.*

List of Symbols and Acronyms

SYMBOLS

$a(n)$	data symbols
$\delta(.)$	Dirac delta function
Δt	time spacing
$(\Delta t)_c$	coherence time
B_c	coherence bandwidth
B_d	Doppler spread
$C(t)$	spreading code
$c_l(.)$	FIR filter coefficient
E_b	energy of a bit
E_s	energy of a symbol
$E\{.\}$	statistical expectation
F_s	sampling frequency
$g_T(.)$	transmitter filter
$g_{MF}(.)$	receiver matched filter
j	imaginary unit ($j = \sqrt{-1}$)
N	block length
N_0	single sided noise PSD
$P(.)$	apriori probability
$p(.\|.)$	conditional probability density function
$\mathrm{Re}\{.\}$	real part
$r(t)$	received signal
$s(t, \mathbf{\Phi})$	baseband transmitted signal

T	symbol interval
T_0	observation interval
T_m	delay spread
T_s	sample interval
$\mathbf{\Phi}$	synchronization parameter vector
$\tilde{\mathbf{\Phi}}$	synchronization parameter trial vector
$\hat{\mathbf{\Phi}}$	estimated synchronization parameter vector
τ	time delay
$\hat{\tau}$	estimated time delay
θ	phase error
$\hat{\theta}$	estimated phase error
$\mu \in [0, 1)$	fractional interval
$\Lambda(.)$	likelihood function
$\Gamma(.)$	log-likelihood function
$\Pi(.)$	rectangular function
$\bigtriangledown(.)$	triangle function
$(.)^*$	complex conjugation
$\|.\|$	absolute value
$\lfloor . \rfloor$	integer part

ACRONYMS

3G	Third Generation Wireless System
3GPP	3rd Generation Partnership Project
ADC	Analog to Digital Converter
AF	Ambiguity Function
AFLT	Advanced Forward Link Trilateration
A-GPS	Assisted Global Positioning System
ANSI	American National Standards Institute
ARIB	Association of Radio Industries and Businesses
BPSK	Binary Phase Shift Keying
BS	Base Station
C/A-Code	Coarse Acquisition Code
CDMA	Code Division Multiple Access

CI	Cell Identity
DA	Data Aided
DD	Decision Directed
DLL	Delay Locked Loop
DoD	Department of Defense
DSP	Digital Signal Processing
DS-SS	Direct Sequence - Spread Spectrum
E-OTD	Enhanced Observed Time Difference
ETSI	European Telecommunications Standards Institute
FCC	Federal Communications Commission
FIR	Finite Impulse Response
GPS	Global Positioning System
IPDL	Idle Period Down Link
GSM	Global System for Mobile Communication
LLF	Log Likelihood Function
LOS	Line Of Sight
MAP	Maximum A Posteriori Probability
ML	Maximum Likelihood
MLE	Maximum Likelihood Estimation
MS	Mobile Station
NCDLL	Non-Coherent Delay Lock Loop
NDA	Non-Data Aided
NLOS	Non-Line Of Sight
OTDOA	Observed Time Difference of Arrival
PAM	Pulse Amplitude Modulation
PLL	Phase Locked Loop
PPS	Precise Position Service
PRN	Pseudo Random Noise
QAM	Quadrature Amplitude Modulation
QPSK	Quadrature Phase Shift Keying
RF	Radio Frequency
sec	Second
SMG	Standard Mobile Group
SNR	Signal-to-Noise Ratio
SPS	Standard Position Service

SWR	Software Radio
SVs	Space Vehicles
TDMA	Time Division Multiple Access
TDOA	Time Difference Of Arrival
TOA	Time Of Arrival
TOT	Time Of Transmission
US	United States
VLSI	Very Large Scale Integration

Chapter 1

Introduction

The high competition between Americans, Asians, and Europeans has led to the coexistence of several radio communication systems and promises a very difficult path towards the convergence to a unique standard wireless mobile system, despite of the benefits of common worldwide standard. This competition introduces new challenges in receiver architecture design to accommodate the different air interfaces. The natural progression of digital radios towards multimode, multistandard terminals is a potential pragmatic solution which is known as the Software Radio (SWR) concept. The main idea is that the radio functionalities of user terminals are defined by software which allows them to dynamically adapt to different radio environments. Even though, the software radio was first introduced for military applications, the digital revolution of electronic systems has enabled software radio to gradually enter also commercial communication systems. The popularity of digital solutions over their analog counterparts resides mainly on their greater flexibility, high integration efficiency, and configurability, as well as on the fast speed at which semiconductor technologies, digital signal processors, and VLSI circuits are developing.

The rapid evolution of communication systems and the new requirements imposed by the standardization authorities have brought various consumer electronics device types and a high demand on new communication services, such as mobile phone positioning with high accuracy. Even if safety was the primary motivation for mobile positioning, a lot of commercial applications have already emerged in the market. For the public interest, mobile phone positioning in a cellular network with reliable and rather accurate position information has become unavoidable after the Federal Communications Commission mandate, FCC-E911 docket on emergency call positioning in USA, and the coming E112 in the European Union [1]. The basic rule of emergency services requires mobile operators to automatically transfer caller location details to the emergency authorities without regard to validation procedures intended to automatic caller identification and localization.

International analysts have also predicted that mobile location services are commercially potential and the most compelling value-added services to the forthcoming third generation mobile systems, taking into consideration the huge range of services that can be provided to the mobile users. Recently, several potential technologies enabling the development of mobile location techniques have emerged and are already competing in the market [2]. A

large number of commercial location-based services are being provided, such as fleet and resource management, vehicle tracking and person to person location and messaging applications [3], [4], location specific traffic information, yacht position, map-based guidance, and navigation [5]. Location based services will allow mobile users to receive personalized and lifestyle-oriented services relative to their geographic location, and provide enormous opportunities for companies and organizations to effectively reach their target groups of strong purchasing power. However, the successful evolution of the mobile location services to a massmarket industry relies mainly on its accuracy, interoperability, end user privacy and availability of attractive services. In view of the sensitivity of location data to the end user privacy and security, appropriate technical solutions that satisfy requirements for security issues must be established to ensure compliance with regulatory rules in this area.

Since the introduction of the software radio concept, several architectures for designing SWR radio platforms have been recently developed through the efforts of commercial and noncommercial organizations [6], [7], [8], [9], [10], [11]. The ultimate goal of designing a single-chip, flexible wireless transceiver supporting multimode and multistandard compatibility introduced new architectures more suitable for integration. The current trend is to push the analog/digital interface towards the antenna to simplify the analog parts and allow the implementation of most receiver functions digitally, increasing therefore the flexibility, configurability, and integrability. As one important functionality, these new receivers require flexible and efficient synchronization algorithms which depend on the system requirements and receiver architecture design.

In digital communication systems, the continuous-time received signal is sampled and these samples are used to make the decisions on the transmitted symbols. The sampling of the received signal must be synchronized to the incoming data symbols. In conventional receivers, the synchronization is performed using a feedback or feed-forward loop to control the phase of the sampling clock which generally requires complicated phase-locked-loop circuits [12]. The new trend of using digital receivers where the sampling of the baseband signal is not synchronized to the incoming data symbols, reduces the analog components since most of the functions are performed digitally [13], [14], [15]. In this receiver architecture, the sampling of the baseband signal is clocked by a free running oscillator, and thus the sampling is not synchronized to the incoming symbols. Therefore, timing adjustment, and in practice also the carrier phase estimation must be done by digital methods after sampling. One way to perform this is to calculate the value of the signal at the desired time instants using interpolation. Maximum likelihood (ML) estimation theory is the basis for coherent theory of synchronization [13]. It provides a general framework for developing near-optimum synchronization schemes for digital communication systems. Joint estimation of signal parameters using the ML approach yields usually to better estimates with respect to the lower bound on the variance, known as the Cramer Rao bound, compared to estimates obtained from separate optimization of the likelihood functions [16].

Another essential receiver functionality closely related to synchronization is the propagation delay estimation which is the basis for positioning technologies. Multipath effects of the mobile channel could degrade the location estimate substantially, and they are regarded as a killer issue in location estimation, and still a challenging topic for research work.

The main goal of the first part of this thesis work is to develop flexible and efficient all-digital synchronization algorithms with good performance and fast convergence. The work focuses on new algorithms for jointly estimating the symbol timing and carrier phase of

digital receivers with non-synchronized sampling clock for both data-aided and non-data-aided systems. To achieve efficient implementation, modest oversampling is used and yet good timing accuracy is achieved by developing low-order polynomial approximations of the likelihood functions. The main emphasis is on the derivation of efficient Farrow-based polynomial approximations of the likelihood function for systematic and practical symbol timing, carrier phase, and fine acquisition frequency synchronization algorithms.

The second main topic is to develop new techniques with subchip resolution capabilities for estimating closely-spaced multipath delays in spread-spectrum CDMA systems in order to estimate correctly the delay of the LOS path. Overlapped closely-spaced multipath components are considered as one of the major sources of error for accurate mobile terminal positioning solutions.

This thesis is organized as follows: In Chapter 2, the polynomial-based maximum likelihood technique for parameter synchronization in digital receivers with non-synchronized sampling clock is established for both DA and NDA systems. Chapter 3 provides an overview of the most promising geolocation solutions, and introduces new techniques for estimating overlapped closely-spaced multipath components. A summary of the main results of this thesis and the author's contribution to the publications are clarified in Chapter 4. The results of this work are given in the publications included in the appendices. Finally, conclusions are drawn in Chapter 5.

Chapter 2

Polynomial-Based ML Technique for Synchronization in Digital Receivers

2.1 INTRODUCTION

In this chapter, new symbol timing and carrier phase estimators are introduced based on ML theory for both data-aided (DA) and non-data-aided (NDA) systems, using a block-based feed-forward architecture. This new technique is a practical, fully digitally implemented synchronization concept using interpolation for jointly estimating the symbol timing and the carrier phase. The interpolation method used in this context is efficiently implemented using the so-called Farrow structure [17] which is characterized by its simple and flexible realization. The likelihood function is expressed in terms of the polynomial coefficients obtained from the Farrow-based interpolator. The feed-forward architecture we are considering provides rapid acquisition characteristics, which are very important especially in the mobile communication systems where the channel characteristics are rapidly changing, and in the case of TDMA system, also the transmission is bursty. Furthermore, the used interpolation approach allows to use modest oversampling (typically twice the symbol rate) while providing the temporal resolution of a highly oversampled system in a computationally efficient manner. In [18], [19], a somewhat similar idea was developed for symbol timing estimation through polynomial approximation of the log-likelihood function. Our approach differs from this earlier idea in that the polynomial approximation of the log-likelihood function is here derived from the piecewise polynomial approximation of the signal in an efficient way. This allows the use of lower sampling rate (oversampling factor of 2 instead of 4). For other approaches to all-digital symbol timing recovery we refer to [14], [15], [20].

This chapter is organized as follows. Section 2.2 discusses briefly the importance of synchronization function and different timing recovery techniques. Section 2.3 gives a brief overview of the maximum likelihood principle for optimum receivers, and presents the typ-

ical likelihood functions required for deriving systematic symbol timing and carrier phase synchronization algorithms. Timing adjustment using polynomial interpolation concept for digital receiver with non-synchronized sampling is reviewed in Section 2.4. The polynomial approximation of the likelihood functions for both DA and NDA systems is derived in Section 2.5. Finally, a summary of the simulation results which are provided in the Publications [P1]-[P5] is presented in Section 2.6.

2.2 SYNCHRONIZATION AND TIMING RECOVERY TECHNIQUES

Synchronization is one of the fundamental functions in communication systems. Its task is to lock the synchronization parameters of the receiver with the received signal. Estimation of synchronization parameters, such as symbol timing, carrier phase and frequency is very essential for performing demodulation and detection of the data from the transmitted signal with high reliability. In conventional receivers, the synchronization is performed using a feedback or feed-forward loop to control the phase of the sampling clock as shown in Fig. 2.1 (a) and (b). These analog and hybrid methods of synchronization are well established in the literature and studied thoroughly [13], [21]. However, their major drawbacks are the large amounts of board space, power consumption, and circuit complexity of phase-locked-loops (PLLs) which are used to control the sampling of incoming signals [12]. Another synchronization method suitable for digital receiver implementation has been introduced during the last decade as shown in Fig. 2.1 (c). In this architecture, the received signal is sampled by a free running clock and thus sampling is not synchronized to the incoming data symbols. Consequently, the synchronization parameters are estimated by digital methods after sampling. This new type of receiver architecture with non-synchronized sampling clock is very relevant to the context of software radio. In fact, existing communication standards are using different data rates, and consequently they employ different master clock rates. In order to reduce the receiver complexity, we can use a single master clock with this receiver architecture and generate the different clock rates virtually by means of sampling rate conversion [10].

The synchronization function is generally very critical to the error performance. Typical examples shown in Figs. 2.2 and 2.3 illustrate the effect of timing offset and phase error on theoretical symbol error probability using QPSK modulation [15], [16].

2.3 MAXIMUM LIKELIHOOD ESTIMATION

In this section, the maximum a posteriori (MAP) and maximum likelihood (ML) estimation criteria are shortly reviewed. Then, the ML criterion is used to device the symbol timing and carrier phase estimators for both DA and NDA systems.

2.3.1 ML Principle for Optimum Receivers

The optimum decision rule to detect the symbol sequence $\mathbf{a}$ in a received signal corrupted by noise is based on the *maximum a posteriori probability* (MAP) estimation criterion, also known as Bayesian estimation [16]. This decision criterion is trying to select the values of

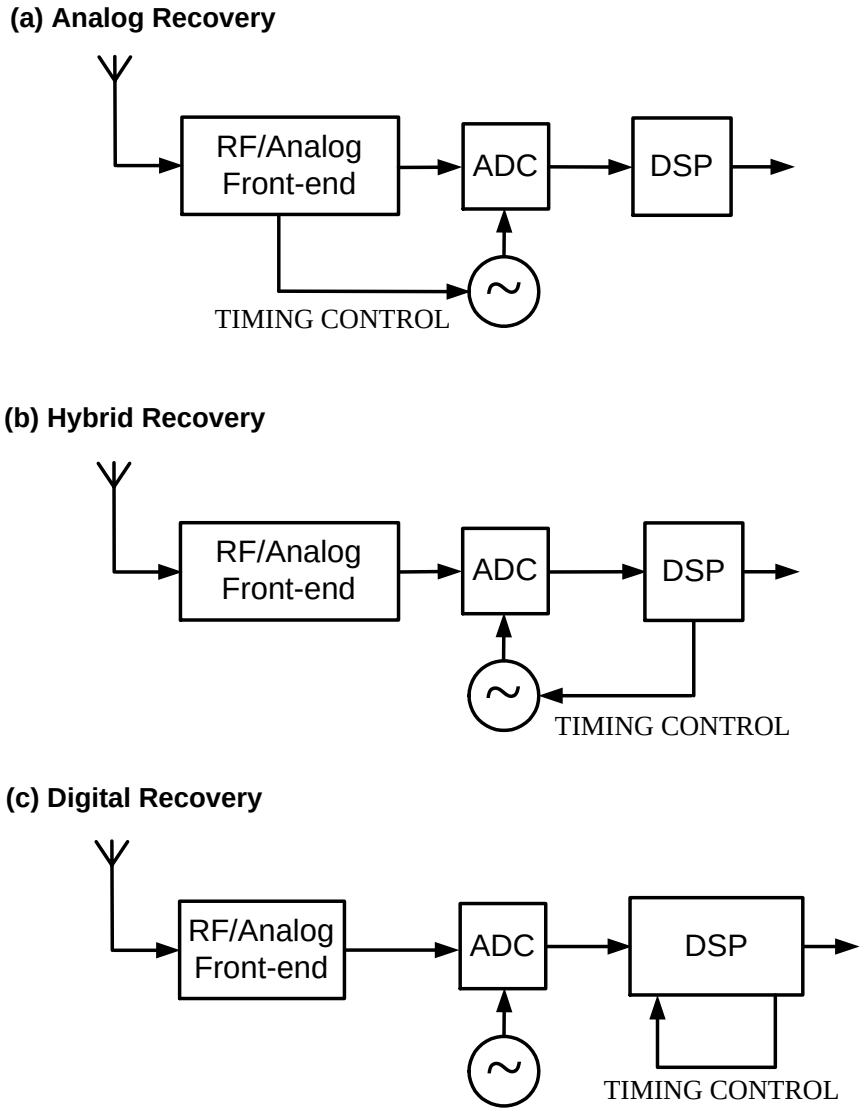

Fig. 2.1 Timing recovery methods.

$\mathbf{a}$ in each transmitted signal interval based on the observation vector $\mathbf{r}$, such that the set of posteriori probabilities is maximized. Under the condition that the prior probabilities are all equal (symbols are uniformly distributed), a detector based on the MAP criterion reduces to the decision criterion based on the maximum of the conditional probability density functions, known as maximum-likelihood (ML) criterion [15].

An optimal ML receiver would perform joint estimation of data $\mathbf{a}$ and synchronization parameters $\mathbf{\Phi} = \{\tau, \theta\}$ simultaneously [20]. Here, τ and θ denote the time delay and carrier phase, respectively. The ML criterion for both data detection and synchronization parameter estimation is trying to select the set of values $\{\hat{\mathbf{a}}, \hat{\mathbf{\Phi}}\}$ which maximizes the likelihood function $p(\mathbf{r}|\mathbf{a}, \mathbf{\Phi})$ as follows

$$(\hat{\mathbf{a}}, \hat{\mathbf{\Phi}}) = \arg \max_{\mathbf{a}, \mathbf{\Phi}} p(\mathbf{r}|\mathbf{a}, \mathbf{\Phi}). \tag{2.1}$$

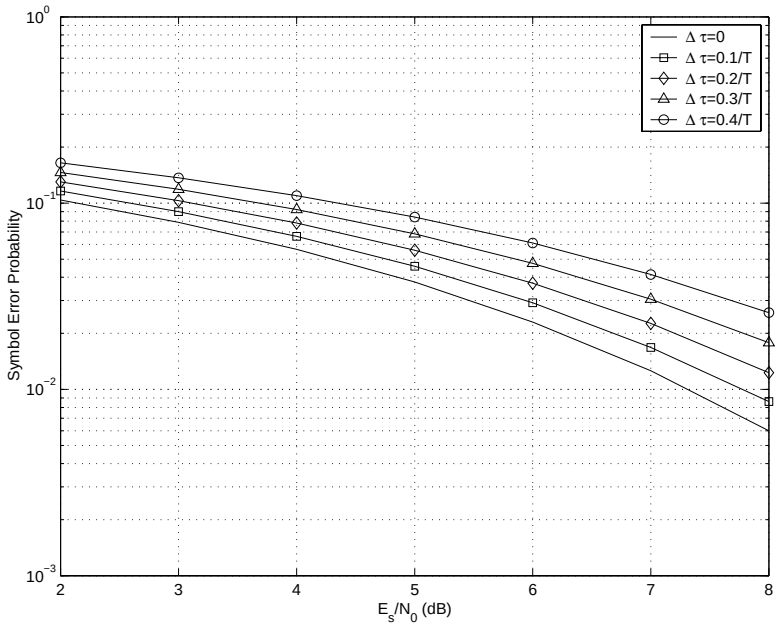

Fig. 2.2 Degradation of symbol error probability due to different timing errors, $\Delta\tau$, using QPSK modulation.

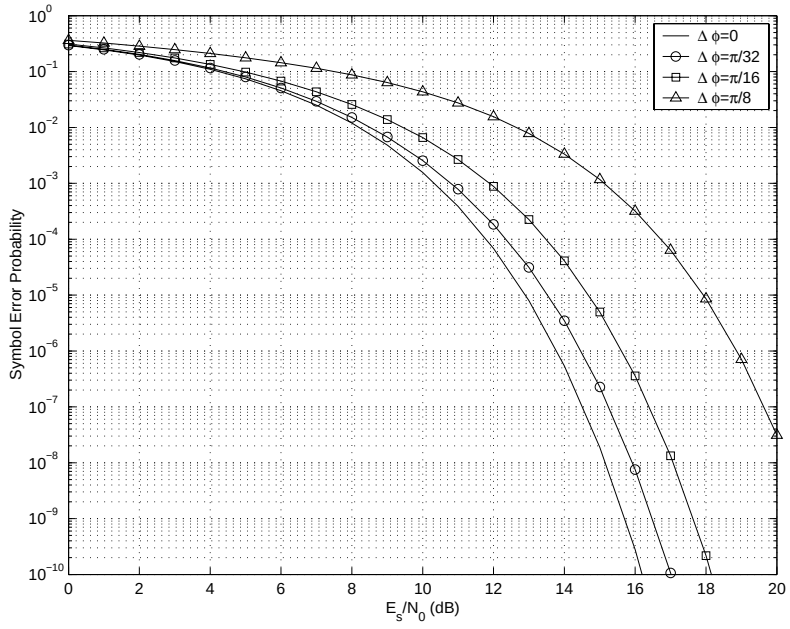

Fig. 2.3 Degradation of symbol error probability due to different phase errors, $\Delta\phi$, using QPSK modulation.

Unfortunately, the optimal joint detection/estimation approach is rather complicated for practical receiver implementation [15], [20]. Therefore, separate data detection algorithms, and independent estimates of each synchronization parameter are commonly derived for re-

alizable receiver structures. Depending on the data dependency, there are three main classes of ML synchronizers:

- The ML data-aided (DA) synchronization algorithms use known data sequence $\mathbf{a}_0$ (preamble, training sequence) at the receiver for the estimation as follows

$$(\hat{\mathbf{\Phi}})^{DA} = \arg \max_{\mathbf{\Phi}} p(\mathbf{r}|\mathbf{a} = \mathbf{a}_0, \mathbf{\Phi}). \tag{2.2}$$

- The ML decision-directed (DD) synchronization algorithms use detected data sequence $\hat{\mathbf{a}}$ instead of the true symbol values for the estimation,

$$(\hat{\mathbf{\Phi}})^{DD} = \arg \max_{\mathbf{\Phi}} p(\mathbf{r}|\mathbf{a} = \hat{\mathbf{a}}, \mathbf{\Phi}). \tag{2.3}$$

- The third class is the ML non-data-aided (NDA) synchronization algorithms. They are using neither the data symbol values nor their estimates. However, they remove the data dependency by averaging over all prior probabilities as follows

$$p(\mathbf{r}|\Phi) = \sum_{\mathbf{a}} p(\mathbf{r}|\mathbf{a}, \mathbf{\Phi}) P(\mathbf{a}). \tag{2.4}$$

  Then, by maximizing the above likelihood function (2.4) with respect to each/all synchronization parameter, the ML NDA algorithms are given by

$$(\hat{\mathbf{\Phi}})^{NDA} = \arg \max_{\mathbf{\Phi}} p(\mathbf{r}|\mathbf{\Phi}). \tag{2.5}$$

2.3.2 Likelihood Function for Systematic Synchronization Algorithms

A linearly modulated transmitted signal in baseband is given by

$$s(t, \mathbf{\Phi}) = e^{j\theta_0} \sum_n a(n) g_T(t - nT - \tau_0), \tag{2.6}$$

where the couple (τ_0, θ_0) are the true values of the unknown clock timing and carrier phase offsets, respectively, $\{a(n)\}$ is the sequence of independent equiprobable data symbols, $g_T(t)$ is the transmitter filter pulse shape, and $1/T$ is the symbol rate.

We assume that $s(t, \mathbf{\Phi})$ is completely known at the receiver except for the synchronization parameter vector $\mathbf{\Phi}$ which consists of the time delay τ and carrier phase θ, and possibly the data symbols. The parameter vector $\mathbf{\Phi}$ is also assumed to remain unchanged over an observation interval T_0 (or sufficiently large number $N = T_0/T$ of transmitted symbols).

The linearly modulated received signal is given by

$$r(t) = s(t, \mathbf{\Phi}) + \eta(t), \tag{2.7}$$

where $\eta(t)$ is an independent white stationary Gaussian noise with flat power spectral density N_0. Recalling the Gaussian nature of the random process, the likelihood function that is to be maximized is given by [15], [16]

$$p(\mathbf{r}|\mathbf{a}, \mathbf{\Phi}) = \xi \exp \left[-\frac{1}{\sigma^2} \int_{T_0} \left| r(t) - \tilde{s}(t, \tilde{\mathbf{\Phi}}) \right|^2 dt \right], \tag{2.8}$$

where ξ is a positive constant, independent of the synchronization parameters which can be neglected, and $\tilde{s}(t, \tilde{\mathbf{\Phi}})$ is the trial local replica generated at the receiver defined by

$$\tilde{s}(t, \tilde{\mathbf{\Phi}}) = e^{j\tilde{\theta}} \sum_n a(n) g_T(t - nT - \tilde{\tau}). \tag{2.9}$$

Maximum likelihood estimation (MLE) is simply trying to minimize the distance between the corrupted received signal $r(t)$ and the trial local replica $\tilde{s}(t, \tilde{\mathbf{\Phi}})$. Equivalently, MLE is trying to estimate one or both values from the parameter set $\hat{\mathbf{\Phi}} = \{\hat{\tau}, \hat{\theta}\}$ using the trial vector $\tilde{\mathbf{\Phi}} = \{\tilde{\tau}, \tilde{\theta}\}$ in order to maximize the likelihood function $p(\mathbf{r}|\mathbf{a}, \mathbf{\Phi})$.

As mentioned earlier, consistent approximations of the above likelihood function are needed to derive systematic ML synchronization algorithms. By expanding the integral in Eq. (2.8), and observing that the energy quantities resulting from the received noisy signal and the local trial signal can be ignored since they are independent of the synchronization parameters, it follows [16]

$$p(\mathbf{r}|\mathbf{a}, \mathbf{\Phi}) \approx \xi \, \exp\left[\frac{2}{\sigma^2} \int_0^{T_0} \mathrm{Re}\Big\{r(t)\, \tilde{s}^*(t, \tilde{\mathbf{\Phi}})\Big\} dt\right]. \tag{2.10}$$

The above approximation is accurate for constant envelope signals (equal symbol energies), e.g., M-PSK, but it is commonly used also for QAM signals.

In the basic system model of Fig. 2.4, after down-conversion to the baseband through mixing and filtering, the received signal is first applied to a receiver matched filter $g_{MF}(t)$, then sampled with a fixed sampling rate $1/T_s$. In practice, the order of sampling and matched filter can be reversed. Under the assumptions that the transmitter and receiver matched filters satisfy the Nyquist properties and the channel is ideal, there is no inter-symbol interference provided that the samples are taken at the correct time instant, i.e., $\tau_0 = \hat{\tau}$. By replacing the local trial signal replica (2.9) in Eq. (2.10), after some manipulations, the likelihood function or objective function becomes [20]

$$\Lambda(\mathbf{a}, \mathbf{\Phi}) = \xi \, \exp\left[\frac{2}{\sigma^2} \mathrm{Re}\Big\{e^{-j\theta} \sum_n a^*(n)\, m(n, \tau)\Big\}\right], \tag{2.11}$$

where $m(n, \tau)$ denotes samples from the output of the matched filter given by

$$m(n, \tau) = \int_0^{T_0} r(t) g_{MF}(nT + \tau - t) dt. \tag{2.12}$$

Taking the logarithm of (2.11) and dropping the resulting constants, we obtain the log-likelihood function (LLF)

$$\Gamma(\mathbf{a}, \mathbf{\Phi}) = \mathrm{Re}\Big\{e^{-j\theta} \sum_n a^*(n)\, m(n, \tau)\Big\}. \tag{2.13}$$

An illustrative example of the likelihood function and its first order derivative is depicted in Fig. 2.5 using QPSK constellation signal and an oversampling factor equal to 50. Several techniques for searching the maximum location of the likelihood function have been devised with a complexity mostly related to the data sample rate and used technology. The

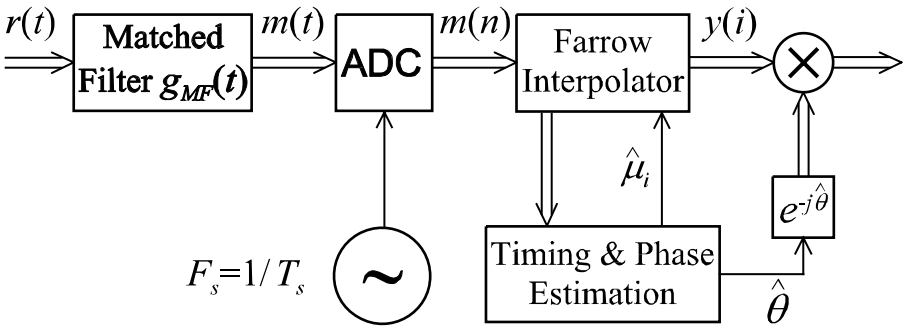

Fig. 2.4 Digital receiver with non-synchronized sampling.

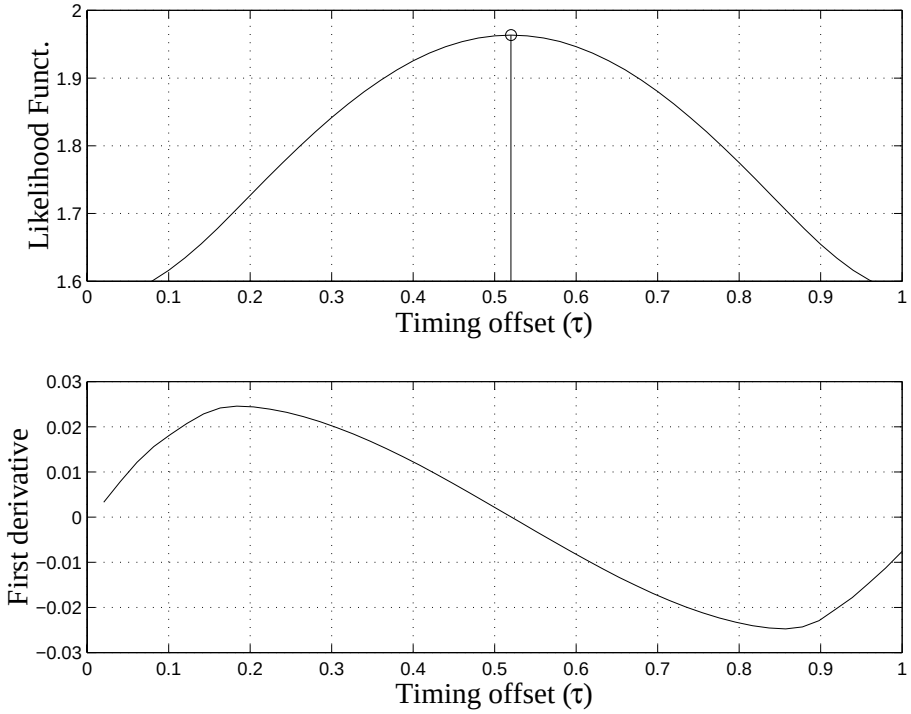

Fig. 2.5 Illustrative example of a typical log-likelihood function for $\tau_0 = 0.52T$ and $\theta_0 = 0$, as well as its first order derivative.

straightforward approach of calculating the log-likelihood function from the discrete-time matched filter output samples would require excessive oversampling factor to achieve sufficient temporal resolution, especially with high-order modulations. Generally, the most straightforward approaches are based on the partial derivatives of the LLF. Namely, the iterative search procedure or the error tracking feedback method [20]. However, the maximum search can be facilitated and optimized using the proposed idea of polynomial-based approximation of the maximum likelihood function.

2.3.3 Data-Aided Estimation

In this case, the symbols $\{a(n)\}$ used for synchronization (preamble, training sequence) are known at the receiver. Similarly, the decision-directed synchronization algorithms use

detected data sequence instead of the true symbol values. For jointly estimating the symbol timing and carrier phase $(\hat{\tau}, \hat{\theta})$, the log-likelihood function has to be maximized with respect to the two parameters τ and θ as follows [15]

$$(\hat{\tau}, \hat{\theta}) = \arg \max_{\tau,\theta} \Gamma(\tau, \theta) \tag{2.14}$$

where the LLF (2.13) can be expressed as

$$\Gamma(\tau, \theta) = \Big| \sum_n a^*(n)\, m(n, \tau) \Big| \, \mathrm{Re}\Big\{ e^{-j\left(\theta - \arg \sum_n a^*(n)\, m(n,\tau)\right)} \Big\}. \tag{2.15}$$

By observing that the magnitude term in Eq. (2.15) is independent of θ, the joint estimation of $(\hat{\tau}, \hat{\theta})$ can be performed by first estimating $\hat{\tau}$ by finding the maximum of the magnitude term

$$\hat{\tau} = \arg \max_{\tau} \Big| \sum_n a^*(n)\, m(n, \tau) \Big| \tag{2.16}$$

and then, the carrier phase estimate $\hat{\theta}$ is easily deduced as

$$\hat{\theta} = \arg \sum_n a^*(n)\, m(n, \hat{\tau}). \tag{2.17}$$

2.3.4 Non-Data-Aided Estimation

Under the assumptions of low SNR and independent equiprobable transmitted data symbols, using quadratic Taylor series expansion of the exponential term in the objective function in Eq. (2.11) and then removing of the data dependency by averaging, the desired approximation of the marginal likelihood function is given by [20]

$$\Lambda(\tau, \theta) = \sum_n E\big[|a(n)|^2\big] \big|m(n, \tau)\big|^2 + \mathrm{Re}\Big\{ \sum_n E[a^2(n)] \big(m^*(n, \tau)\big)^2 e^{-2j\theta} \Big\}. \tag{2.18}$$

Detailed mathematical derivations of the above marginal likelihood function are provided in [20], Chapter 5.

Consequently, for a uniformly distributed phase, the likelihood function of Eq. (2.18) is reduced to

$$\Lambda(\tau) = \sum_n \big|m(n, \tau)\big|^2. \tag{2.19}$$

Hence, the NDA timing estimate for any linear digital modulation is given by [15]

$$\hat{\tau} = \arg \max_{\tau} \sum_n \big|m(n, \tau)\big|^2. \tag{2.20}$$

For M-PSK signalling, joint symbol timing and carrier phase estimate is feasible and carrier phase estimate is given by

$$\hat{\theta} = \frac{1}{M} \arg \sum_n \big(m(n, \hat{\tau})\big)^M. \tag{2.21}$$

2.4 TIMING ADJUSTMENT USING POLYNOMIAL INTERPOLATION

This section reviews and demonstrates how the symbol timing adjustment can be done digitally using an interpolator if the sampling of the receiver signal is not synchronized to the symbol timing instants. It is also discussed how the polynomial-based interpolation methods can be efficiently implemented using the so-called Farrow structure. In the next section, the polynomial-based interpolation and the Farrow structure are utilized to derive the proposed ML based symbol timing and carrier phase estimation algorithm.

2.4.1 Receiver with Non-Synchronized Sampling

In this work we consider the receiver structure where the sampling is done using a fee-running oscillator and the symbol timing and carrier phase estimation and correction are done completely in the digital part of the receiver, as shown in Fig. 2.4. Here the received baseband signal after the matched filter, denoted by $m(t)$, is sampled using the over-sampling ratio of $\beta = T/T_s$, where T and T_s are the symbol and sampling intervals, respectively. In the digital part of the receiver, the timing error $(\hat{\tau}_i)$ and phase error $(\hat{\theta})$ are estimated (to be discussed in the next section) and the symbol timing adjustment is done first using interpolator and, after that, the phase error is corrected using a phase rotator.

For convenience, it is assumed that the ADC sampling rate is an integer multiple of the symbol rate, and the interpolator output sampling rate is equal to the symbol rate. In this case, the fractional interval is constant, $\mu_i = \mu$, in stationary conditions. The fractional interval and timing offset are related as follows:

$$\mu = \frac{\tau}{T_s} - \left\lfloor \frac{\tau}{T_s} \right\rfloor \qquad \text{where} \quad \mu \in [0, 1). \tag{2.22}$$

Here, $\lfloor x \rfloor$ stands for the integer part of x.

2.4.2 The Farrow Structure

It has turned out that the polynomial-based interpolation methods are the most widely used solution for performing the symbol timing adjustment in digital receivers. The reason for the popularity of these methods lies in the fact that interpolator can then be efficiently implemented using the Farrow structure [17]. This filter structure, shown in Fig. 2.6, consists of $L+1$ parallel FIR filters having the transfer functions $C_l(z)$ for $l = 0, 1, \cdots, L$. Here L denotes the degree of the polynomial interpolation. The impulse response of the interpolator in each T_s-segment with basepoints $k = I_1$ to I_2:

$$h(t) = h(iT) = h[(k + \hat{\mu}_i)T_s] = \sum_{l=0}^{L} c_l(k)\hat{\mu}_i^l \tag{2.23}$$

with $c_l(k)$'s being the fixed coefficients of the FIR filters of length $I_2 - I_1 + 1$.

The synchronized output samples of this structure are be given by

$$y(i) = \sum_{k=I_1}^{I_2} m(n_i - k)h[(k + \hat{\mu}_i)T_s] = \sum_{l=0}^{L} v_l(n_i)\hat{\mu}_i^l, \tag{2.24}$$

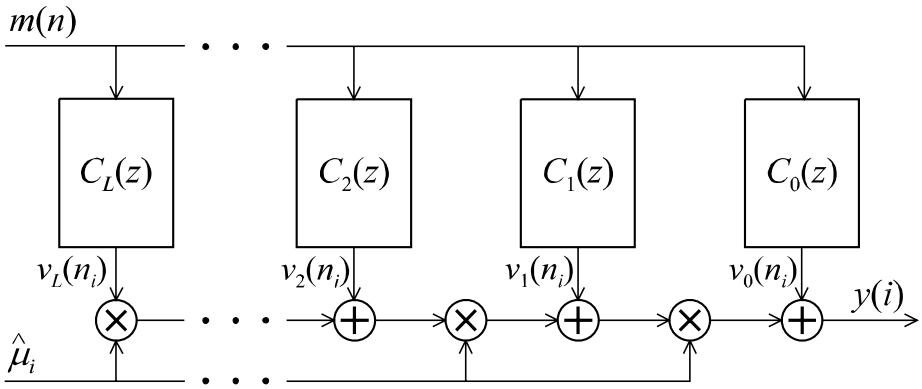

Fig. 2.6 The Farrow structure for polynomial-based interpolation filter.

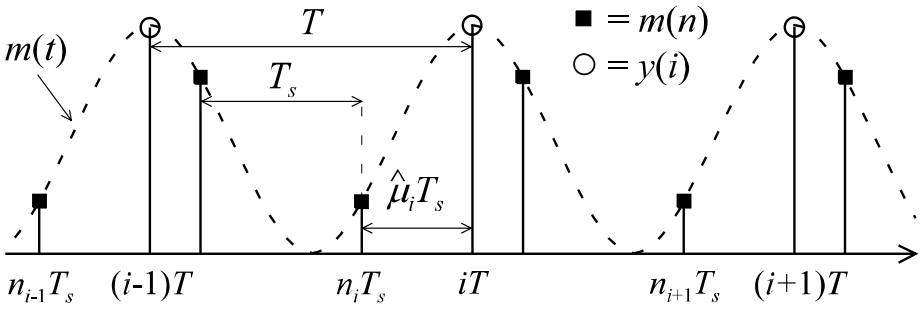

Fig. 2.7 Example of the input and output samples for the Farrow structure. Here the over-sampling ratio is $\beta = T/T_s = 2$.

where

$$v_l(n_i) = \sum_{k=I_1}^{I_2} m(n_i - k)c_l(k). \tag{2.25}$$

The FIR filter coefficients for the Lagrange interpolation are given, e.g., in [14] and for more general interpolation techniques, see [17], [22], [23].

The idea of the Farrow structure is that the output samples of the FIR filters $v_l(n_i)$ as given by Eq. (2.25) form a polynomial approximation for the continuous-time signal $m(t)$ in the interval $n_iT_s \leq t < (n_i + 1)T_s$. The output sample $y(i)$ is then calculated by evaluating the value of the polynomial at the time instant determined by $\hat{\mu}_i$ according to Eq. (2.24). Therefore, the time instant for the output sample $y(i) = y(iT)$ is determined by (see Fig. 2.7)

$$iT = (n_i + \hat{\mu}_i)T_s \qquad \text{with} \quad 0 \leq \hat{\mu}_i < 1. \tag{2.26}$$

The advantage of the Farrow structure is that the filter coefficients $c_l(k)$ are fixed and the time instant for the output sample can be easily controlled by the fractional interval $\hat{\mu}_i$.

2.5 POLYNOMIAL APPROXIMATION FOR THE LOG-LIKELIHOOD FUNCTION

In this section, we derive the polynomial approximation for the log-likelihood function for both DA and NDA cases. We consider the case of a non-synchronized receiver where the sampling rate is twice the symbol rate ($T = 2T_s$), consequently, we are going to use τ and μ in the following to denote the timing error as fractions of the symbol and sampling interval, respectively. The function of the interpolation filter is to calculate the correct output sample, $y(i) = y(iT)$, at a time using a set of adjacent input samples, $m(n) = m(nT_s)$, obtained from the output of the matched filter based on a timing error estimate $\hat{\mu}$. Here n denotes the largest integer for which $nT_s \leq iT$.

2.5.1 Data-Aided Estimator

In the following, the polynomial approximation for the log-likelihood function is derived by utilizing the fact that the output samples of the FIR filters in the Farrow structure, denoted by $v_l(n)$, form an L^{th} order polynomial approximation for the input signal $m(n)$. This approximation is piecewise polynomial, i.e., there are different polynomial approximations for each sample interval. Because we are using two samples per one symbol interval, there are two different polynomial approximations of the log-likelihood function [P2] corresponding to the two halves of the symbol interval. Consequently, from expression (2.16) the symbol timing is estimated by

$$\hat{\tau} = \arg\max_{\tau} \begin{cases} |\Gamma_1(2\tau)| & \text{for } 0 \leq \tau < T/2 \\ |\Gamma_2(2\tau - 1)| & \text{for } T/2 \leq \tau < T \end{cases} \tag{2.27}$$

where the LLF functions $\Gamma_1(2\tau)$ and $\Gamma_2(2\tau - 1)$ are generated using odd and even samples of the matched filter output $m(n, \tau)$, as follows

$$\begin{cases} \Gamma_1(2\tau) = \sum_{n=1}^{N} a^*(n) m(2n - 1, 2\tau) & \text{for } 0 \leq \tau < T/2 \\ \Gamma_2(2\tau - 1) = \sum_{n=1}^{N} a^*(n) m(2n, 2\tau - 1) & \text{for } T/2 \leq \tau < T. \end{cases} \tag{2.28}$$

Also, by using the timing estimate $\hat{\tau}$ in the corresponding symbol time interval, the carrier phase estimate (Eq. (2.17)) becomes

$$\hat{\theta} = \begin{cases} \arg \Gamma_1(2\hat{\tau}) & \text{for } 0 \leq \hat{\tau} < T/2 \\ \arg \Gamma_2(2\hat{\tau} - 1) & \text{for } T/2 \leq \hat{\tau} < T. \end{cases} \tag{2.29}$$

The above expressions can be rewritten with respect to the sample interval denoted here by the fractional interval μ. The LLF equation (2.28) becomes

$$\begin{cases} \Gamma_1(\mu T_s) = \sum_{n=1}^{N} a^*(n) m(2n - 1, \mu T_s) \\ \Gamma_2(\mu T_s) = \sum_{n=1}^{N} a^*(n) m(2n, \mu T_s). \end{cases} \tag{2.30}$$

The values of $m(n, \mu T_s)$ can be interpolated for different values of $\mu \in [0, 1)$ by utilizing the Farrow structure and the original samples $m(n)$. Thus, the interpolated sample values

expressed as a function of the FIR branch filter outputs in the Farrow structure, $v_l(n)$, and the fractional interval, μ, are given by [P2]

$$\begin{cases} m(2n-1,\mu T_s) = \sum_{l=0}^{L} v_l(2n-1)\mu^l \\ m(2n,\mu T_s) = \sum_{l=0}^{L} v_l(2n)\mu^l. \end{cases} \tag{2.31}$$

where L is the degree of polynomial approximation. Finally, by substituting Eq. (2.31) into (2.30), the polynomial approximation of the log-likelihood function can be written as:

$$\begin{cases} \Gamma_1(\mu T_s) = \sum_{l=0}^{L} \left(\sum_{n=1}^{N} a^*(n) v_l(2n-1) \right) \mu^l \\ \Gamma_2(\mu T_s) = \sum_{l=0}^{L} \left(\sum_{n=1}^{N} a^*(n) v_l(2n) \right) \mu^l. \end{cases} \tag{2.32}$$

Consequently, the symbol timing and the carrier phase estimation can be performed easily with the aid of the Farrow structure. First, the polynomial coefficients of the log-likelihood functions are calculated by averaging the product of $a^*(n)$ and $v_l(n)$ over N symbols according to Eq. (2.32). It has turned out through simulations that the values of N between 16 and 64 provides good results. Second, the value of the timing error estimate $\hat{\mu}$ that maximizes either of the log-likelihood functions $\{\Gamma_1(\mu T_s), \Gamma_2(\mu T_s)\}$ is computed. Finally, by using the timing estimate, the carrier phase estimate $\hat{\theta}$ is calculated. A formal description of this algorithm is written as follows:

If $\max|\Gamma_1(\mu T_s)| > \max|\Gamma_2(\mu T_s)|$ **then**
$\hat{\mu} = \arg\max_{\mu} |\Gamma_1(\mu T_s)|$
$\hat{\theta} = \arg[\Gamma_1(\hat{\mu} T_s)]$
else
$\hat{\mu} = \arg\max_{\mu} |\Gamma_2(\mu T_s)|$
$\hat{\theta} = \arg[\Gamma_2(\hat{\mu} T_s)]$
end If

The overall scheme of the proposed DA block-based symbol timing and carrier phase recovery is illustrated in Fig. 2.8. After the parameters $\hat{\mu}$ and $\hat{\theta}$ are estimated, timing adjustment is performed by evaluating the value of the polynomial at the given value of $\hat{\mu}$. Subsequently, the carrier phase is corrected by the factor $e^{-j\hat{\theta}}$.

The efficiency of this algorithm is due to the fact that here the block averaging of the likelihood function is done in the polynomial coefficient domain, and the multiplications with $\hat{\mu}$ are needed only for the whole estimation block. The above procedure can be used as such in the data-aided (DA) systems where the symbol values are known in advance. For example, GSM does have a known synchronization symbol sequence. In case of decision-directed (DD) systems, a reasonably good initial estimate for the sampling phase must be known. This scheme can also be utilized in non-data-aided (NDA) systems with some modifications as shown in the following section.

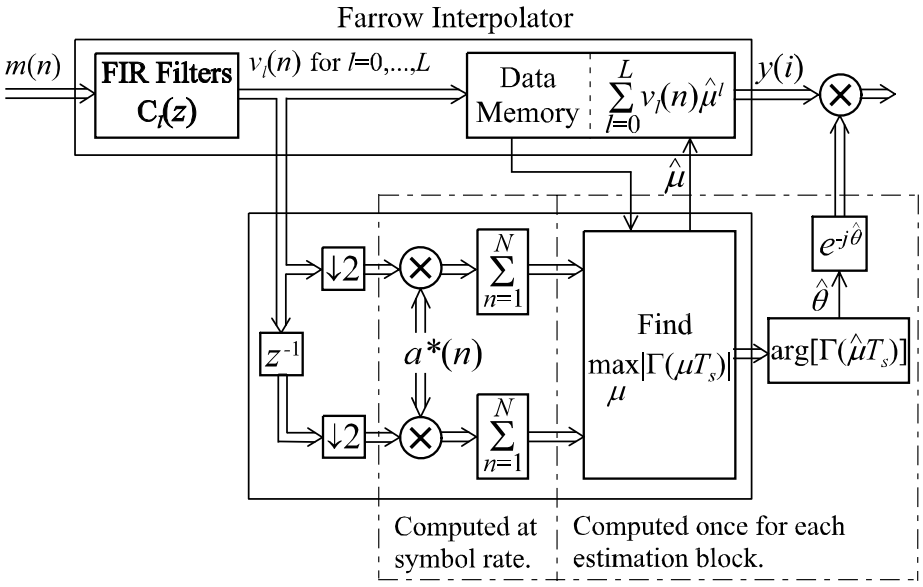

Fig. 2.8 DA symbol timing and carrier phase synchronization scheme.

2.5.2 Non-Data-Aided Estimator

Similarly to the DA estimators, the symbol timing for the NDA case is derived from expression (2.20) as follows [P3]

$$\hat{\tau} = \arg\max_{\tau} \begin{cases} \Lambda_1(2\tau) & \text{for } 0 \le \tau < T/2 \\ \Lambda_2(2\tau - 1) & \text{for } T/2 \le \tau < T \end{cases} \tag{2.33}$$

where the likelihood functions $\Lambda_1(2\tau)$ and $\Lambda_2(2\tau - 1)$ are given by

$$\begin{cases} \Lambda_1(2\tau) = \sum_{n=1}^{N} \left| m(2n-1, 2\tau) \right|^2 & \text{for } 0 \le \tau < T/2 \\ \Lambda_2(2\tau - 1) = \sum_{n=1}^{N} \left| m(2n, 2\tau - 1) \right|^2 & \text{for } T/2 \le \tau < T. \end{cases} \tag{2.34}$$

The likelihood functions (2.34) can also be expressed as a function of the fractional interval and interpolation filter branches as follows;

$$\begin{cases} \Lambda_1(\mu T_s) = \sum_{n=1}^{N} \left| \sum_{l=0}^{L} v_l(2n-1)\mu^l \right|^2 \\ \Lambda_2(\mu T_s) = \sum_{n=1}^{N} \left| \sum_{l=0}^{L} v_l(2n)\mu^l \right|^2. \end{cases} \tag{2.35}$$

The carrier phase estimate for an M-PSK signal is deduced by using the above timing estimate $\hat{\tau}$, as follows

$$\hat{\theta} = \begin{cases} \frac{1}{M} \arg \sum_{n=1}^{N} \left(\sum_{l=0}^{L} v_l(2n-1)\hat{\mu}^l \right)^M \\ \frac{1}{M} \arg \sum_{n=1}^{N} \left(\sum_{l=0}^{L} v_l(2n)\hat{\mu}^l \right)^M. \end{cases} \tag{2.36}$$

By noticing that the summation inside the parentheses is actually the output sample of the Farrow structure $y(i)$ for both $0 \le \tau < T/2$ and $T/2 \le \tau < T$, Eq. (2.36) can be rewritten

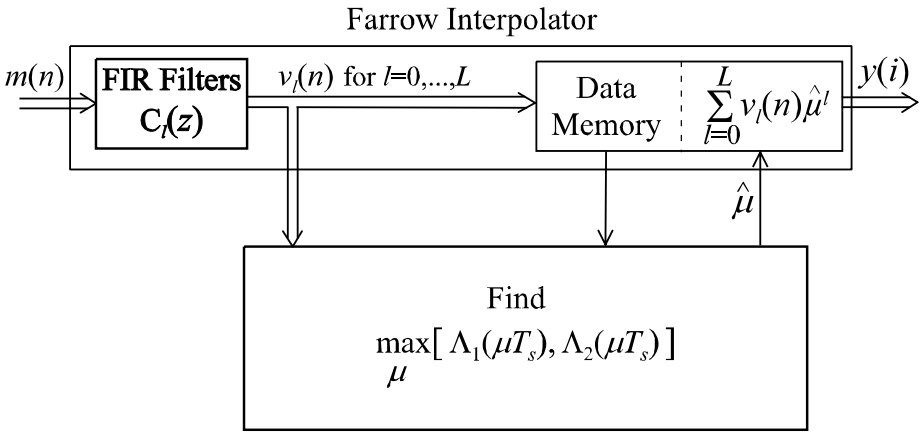

Fig. 2.9 NDA symbol timing recovery scheme.

as

$$\hat{\theta} = \frac{1}{M} \arg \sum_{n=1}^{N} \big(y(i)\big)^M. \tag{2.37}$$

Finally, the symbol timing estimate is reduced to the search of the value of $\hat{\mu}$ that maximizes either of the likelihood functions $\{\Lambda_1(\mu T_s), \Lambda_2(\mu T_s)\}$. Then, the timing estimate is used for computing the carrier phase estimate $\hat{\theta}$. Alternatively, this algorithm is described as follows;

If $\max[\Lambda_1(\mu T_s)] > \max[\Lambda_2(\mu T_s)]$ **then**
$\hat{\mu} = \arg\max_{\mu}[\Lambda_1(\mu T_s)]$
$\hat{\theta} = \frac{1}{M} \arg \sum_{n=1}^{N} \big(y(i)\big)^M$
else
$\hat{\mu} = \arg\max_{\mu}[\Lambda_2(\mu T_s)]$
$\hat{\theta} = \frac{1}{M} \arg \sum_{n=1}^{N} \big(y(i)\big)^M$
end If

The overall scheme of the NDA block-based symbol timing and carrier phase recovery is illustrated in Figs. 2.9 and 2.10. Notice that the influence of the data symbols of this NDA feed-forward phase estimator is removed by the M^{th} power. Remark also that in this case, the averaging of the likelihood function cannot be done in the polynomial coefficient domain. Consequently, the algorithm is not as efficient as in the DA case with respect to the computational complexity.

2.6 SUMMARY OF SIMULATION RESULTS

Simulations have been performed to analyze the performance of digital receivers with non-synchronized sampling using the proposed polynomial-based ML synchronization algorithms for both DA and NDA cases and the results are shown in the publications [P1]-[P5]. The proposed schemes are simulated using an AWGN channel model, and different signal constellation types (i.e., PAM, QPSK, 16-QAM, and 64-QAM) for different block lengths

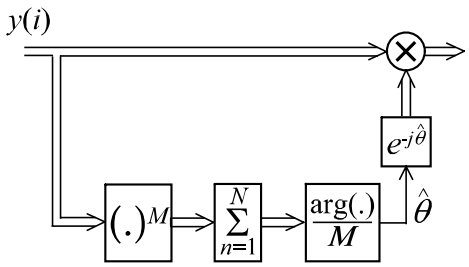

Fig. 2.10 NDA carrier phase estimation scheme for M-PSK modulations.

N. The transmitter and receiver pulse-shaping filters are square root raised cosine filters with excess bandwidth of 35%.

A frequency domain optimized third order interpolation filter $(L = 3)$ of length 8 designed by using a minimax synthesis technique [24] is compared in the simulations with the conventional cubic Lagrange interpolator [13]. The length of the FIR filters in the Farrow structure for the optimized interpolator is twice as long as for the Lagrange interpolator. However, the filter coefficients are symmetrical for this optimized design which makes its complexity of the same order with the Lagrange interpolator. The number of the FIR filter branches is four for both interpolators. Also, the simulations are done using the worst-case timing offset and some selected values of the phase error.

Several sets of experiments have been conducted for both DA and NDA synchronization approaches. Theoretical expectations are compared with simulated worst case (with respect to timing offset) SEP as a function of E_b/N_0 using different types of modulations. Also, variance and mean of the timing jitter as well as symbol error probability (SEP) of both interpolators are compared. The effect of a relatively small frequency error, compared to the symbol rate, on the synchronization scheme is analyzed in [P4]. The simulation results demonstrate the efficiency and excellent performance of the proposed block-based feedforward estimators even in the presence of a small frequency error. Also, the results show the excellent performance of the frequency domain optimized interpolator compared to the traditional Lagrange interpolator specially if we want to make use of shorter block lengths which provide fast acquisition. In [P5], a new frequency estimator for fine acquisition suitable for this digital reciever type is derived. The simulation results of this work are given in the publications [P1]-[P5] included in the appendices, and a summary of the main results is presented in Chapter 4.

Chapter 3

Multipath Delay Estimation for Accurate Positioning

3.1 INTRODUCTION

In this chapter, we provide an overview of the most promising geolocation positioning techniques for wireless systems that are being standardized, including a survey of fundamental concepts and major problems in positioning. Then we briefly review the GPS system. Finally, we discuss and introduce new techniques with subchip resolution capabilities for estimating closely-spaced multipath delays in spread spectrum CDMA systems. Generally, multipath delays caused by distant reflectors have relatively large delay spread, more than one chip interval, that can be detected using conventional techniques [25], [26]. However, shorter excess path delays result in overlapped fading multipath components that introduce significant errors to the LOS path time and gain estimation. The proposed algorithms are intended to improve the accuracy of location estimates of GPS, as well as, mobile phone positioning using the cellular network assisted GPS technology by estimating correctly the LOS path. In the sequel, we will focus our study mainly on the GPS case.

3.2 TECHNIQUES FOR PERSONAL POSITIONING: PRINCIPLES AND PROBLEMS

Although mobile location is an enhanced feature of cellular systems which are primarily designed only for voice and data transmission, there exist some basic parameters available to the network that can be used to generate a rough position estimate. These available pieces of information, such as serving cell identity (CI), timing advance, and measured signal strengths of the serving and neighboring cells, can provide only a limited precision of location which cannot in any case satisfy the FCC requirements [1]. Even though, mobile positioning is a rather new concept and it is still in its infancy, various geolocation technologies have been recently devised using either *cellular network-based*, *mobile-based*,

or *hybrid* approaches [2]. Hereafter, we briefly discuss the most prominent positioning methods that have been approved for standardization within the 3^{rd} Generation Partnership Project (3GPP)[1], by the sub-committee T1P1.5 of the American T1 Standards Committee, and subsequently in ETSI Technical Committee SMG. The methods that are being standardized by T1P1.5 for GSM are Time of Arrival (TOA), Enhanced Observed Time Difference (E-OTD), and Assisted GPS (A-GPS) [27]. In addition, Observed time difference of Arrival - Idle Period Down Link (OTDOA-IPDL) and Cell Identity methods have been added to allow easy migration to the upcoming 3G systems [28].

- **Time of Arrival**

  Time of Arrival positioning method with known time of transmission (TOT), is a multilateral and pure network-based approach where multiple base stations listen to handover access bursts and triangulate the position of the mobile. Measurements of the exact time of arrival of at least three MS to BSs radio links has to be performed with respect to a synchronized and common reference time clock [53]. The location of the user equipment is consequently given by the intersection of the three TOA circles. TOA positioning requires full network synchronism, which is not the case for GSM and the forthcoming 3G networks [2].

  A more practical and suitable technique for the asynchronous networks is the *Time Difference of Arrival* (TDOA) positioning where TOA differences are used in order to eliminate the unknown TOT from the observations. TDOA technique relies simply on the time difference at which signal arrives at multiple BSs, rather than on the absolute arrival time like the TOA method [29]. TOA estimates of a serving BS and its neighbor yield one TOA difference which result in a hyperbola that lies between the two BSs. Measurements of TOA from at least four serving neighbor BSs result in three hyperbolas. The intersection of the three hyperbolas determines the mobile device position, and this is known as hyperbolic trilateration [29].

- **Enhanced Observed Time Difference**

  Enhanced Observed Time Difference is basically reversed TOA or mobile terminal based TOA, where the handset is much more actively involved in the positioning process. E-OTD is a unilateral approach that involves the mobile station in estimating the timing differences between the various base stations [30]. In E-OTD, the mobile station listens to bursts from several base stations and measures the observed time differences, which are then used for trilateration of the mobile position as shown in Figure 3.1.

  Unilateral E-OTD principle has been approved for standardization in different cellular systems. For GSM it is called E-OTD, in 3G systems it is OTDOA-IPDL, and in US-CDMA it is called Advanced Forward Link Trilateration (AFLT). These systems have different names mainly because of the different network types and measurement processes of TOA signals [27].

- **Assisted Global Positioning System (A-GPS)**

[1]3GPP is a joint activity of the European ETSI, American National Standards Institute, and Japanese ARIP to standardize next generation wireless communication systems.

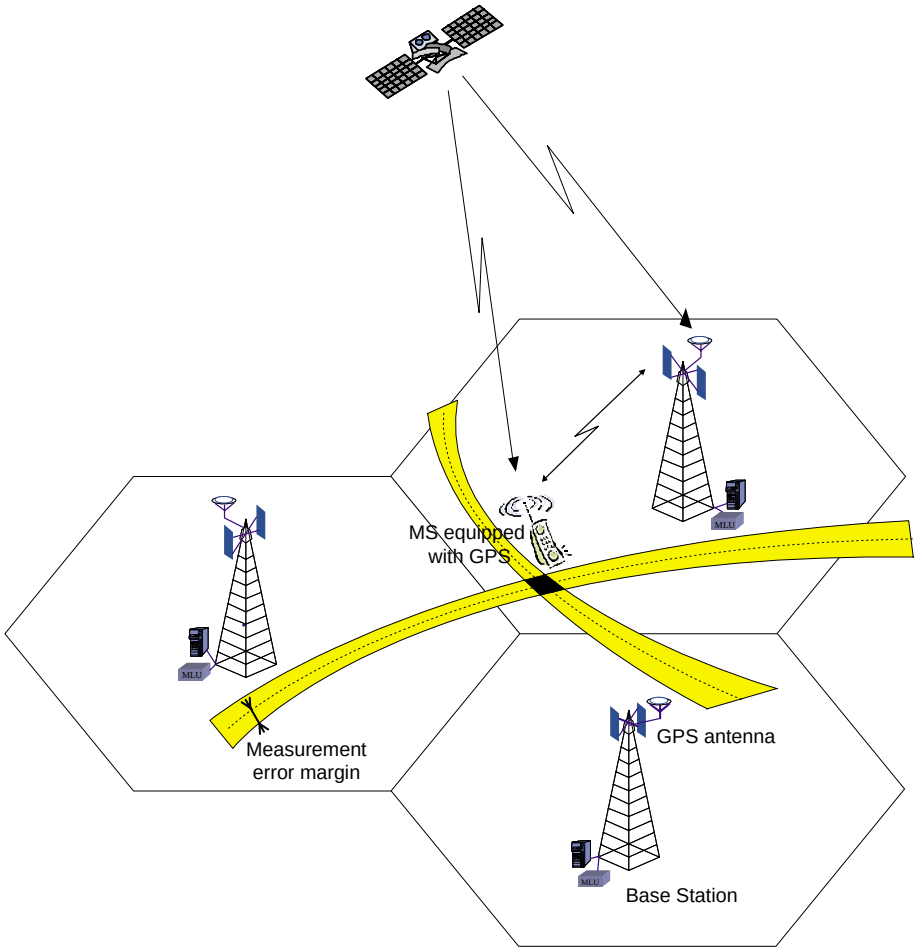

Fig. 3.1 Principles of E-OTD and A-GPS methods in cellular network.

Assisted Global Positioning System relies on mobile stations having an integrated GPS receiver aided by the cellular network assistance and support to enhance the positioning, especially for the non-line-of-sight (NLOS) conditions and indoor environments. Assistance data is transmitted from the network to the MS in order to expedite the GPS signal acquisition search and therefore shortening the time-to-first-fix from minutes to a second or less [31]. GPS-based positioning appears to be the most prominent and the leading candidate for wireless systems in terms of accuracy, reliability, latency, availability, and continuity of service [2].

The major problem of the above described geolocation solutions, with the exception of A-GPS, is that they are unable to deliver reliable positioning to the end user with homogeneous performance in urban, suburban, rural, and indoor environments. Currently, the efforts are aiming at defining hybridised solutions that satisfy all the imposed requirements, involving the lowest possible cost and minimal impact on the network and handset equipment. For example, network-based positioning systems have the advantage of working with all existing mobiles, but have the disadvantage of limited accuracy and requiring additional investments in the supporting infrastructure. Similarly, mobile station based on stand-alone GPS provides location capability with high accuracy, also in the absence of wireless coverage or network assistance using the same infrastructure, but requires handset modifications,

receiver could take several minutes to acquire the satellite signals, and generally fails in radio shadows and indoor environments.

Another major source of error that has a strong impact on the accuracy of most geolocation solutions, including GPS, is due to the multipath signal propagation that may be due to atmospheric reflection or refraction, or reflections from buildings and other objects. Commonly, in most applications of radio communications and navigations [25], the line of sight (LOS) signal is succeeded by multipath components that arrive at the receiver within a short delay spread, that can be less than one chip interval. This causes overlapping fading multipath components and introduces significant errors in the LOS path time of arrival and gain estimation. In spread spectrum CDMA systems, such as third generation mobile communications or GPS receivers, it is important to achieve accurate delay estimation (or code synchronization) before despreading and data detection. Also, most spread spectrum systems use spreading codes with non-ideal correlation properties which result in co-channel interference, or multiuser-interference, for radio communication systems, which is also called multi-transmitter interference in radio-navigation systems [25]. Generally, the performance of radio communication systems is heavily affected by the multipath and multiuser-interferences.

3.3 FUNDAMENTALS OF GPS

The principle of GPS positioning is based on the concept of TOA ranging to determine the user location. This concept entails measuring the propagation time of signals broadcast simultaneously from satellites at known locations. Ideally, the distance between a satellite and a user receiver is obtained by multiplying the propagation-time (or transit-time) with the speed of light. The GPS satellites, or space vehicles (SVs), are put in medium earth orbital planes and they are moving in space at a speed of about 4 km/s along their orbits, repeating almost the same ground track once each day. Although each SV is equipped onboard by a pair of ultra-stable atomic clocks, the satellite clocks are maintained in synchronism by the monitoring control segment that uploads the updated parameters for each SV clock, together with the navigation message broadcast by each satellite [32].

In theory, a receiver can estimate its position using three TOA measurements if the satellite and receiver clocks are synchronized. However, in practice the user's receivers typically employ inexpensive and low-accuracy quartz oscillators as local clocks, which are set approximately to GPS time. Therefore, the receiver clock introduces certain timing offset or clock-bias to the true GPS time which affects the observed transit-time for all satellites equally. The receiver can overcome this problem by measuring the distance to four SVs in view. These measured distances are usually too short, or too long, compared to the 'real' range by a common amount and they are called pseudo-ranges. In addition to the 3-dimensional coordinates of spatial position, a user needs to estimate the receiver clock offset. The user position can then be determined by solving the four pseudo-ranges for the four unknowns [33].

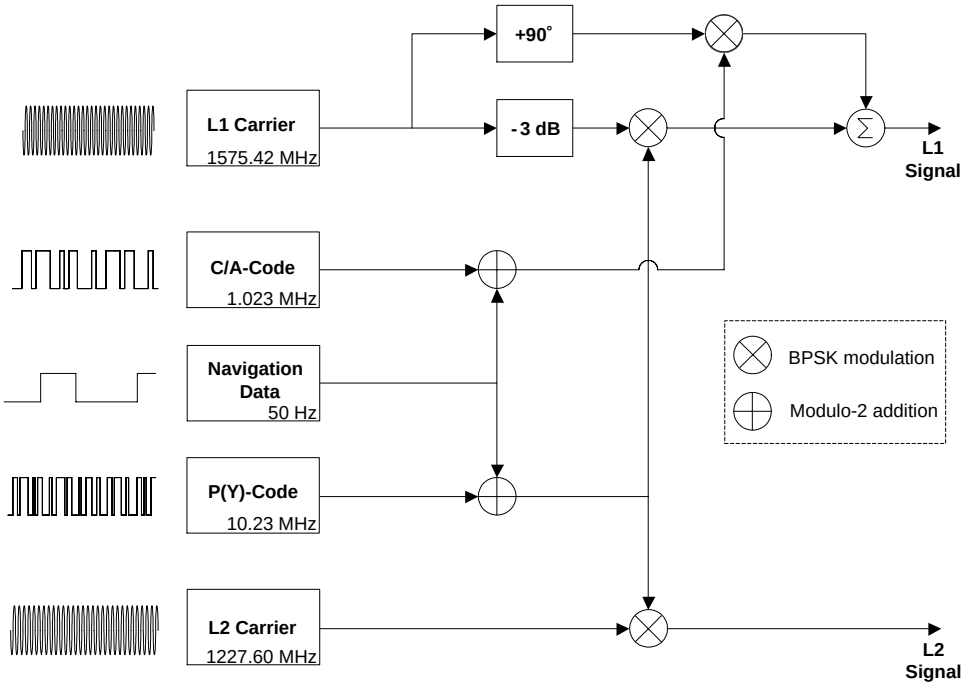

Fig. 3.2 GPS signal structure.

3.3.1 Satellite Signals

GPS satellite transmissions utilize direct sequence spread spectrum (DS-SS) modulation [32]. Spread spectrum techniques have been widely in military use because they can combat strong interference and prevent message recovery by unauthorized receivers, and they have also been adopted for commercial applications [16]. Spread spectrum communication systems involve the transmission of a signal in a radio frequency bandwidth much greater than the data information bandwidth to be conveyed. These systems spread the transmitted signal spectrum over a frequency range substantially greater than the bandwidth of the modulating data message. In Direct sequence (DS) systems, the spectral spreading is performed by multiplying the data signal by an auxiliary pseudo random-noise (PRN) code [34].

Each SV broadcasts two types of PRN ranging signals, as well as navigation data which consists of satellite ephemeris data and satellite health data, allowing users to measure their pseudo-ranges and hence estimating their positions, velocity, and time [32]. Figure 3.2 illustrates the GPS signal structure. The ranging signals are pseudo-random noise codes that modulate the satellite carrier frequencies using binary phase shift keying (BPSK). Each satellite transmits continuously two microwave carrier signals called the primary carrier, $L_1 = 1575.42$ MHz, and secondary carrier, $L_2 = 1227.60$ MHz. The carrier frequencies are modulated by spread spectrum codes with a unique PRN sequence associated to each satellite and by the navigation data [33]. The near orthogonality of the PRN code sequences permits all the satellites to transmit on the same carrier frequencies without incurring significant mutual interference [34]. PRN codes are simply deterministic binary sequences with specific statistical random noise-like properties [34]. The family of PRN codes is mainly characterized by the low cross-correlation between the codes, they are nearly orthogonal, and the autocorrelation function is almost zero except at zero delay [32].

3.3.2 Signal Characteristics

The carrier frequency L_1 is BPSK modulated by two PRN codes, the coarse acquisition code (C/A-code) and the precision code (P-code), while L_2 is BPSK modulated only by the P-code. Low rate navigation data is modulated to both carriers. The P-code is available only for USA Department of Defense (DoD) authorized users and, when encrypted, is called Y-code. P-code is a very long PRN code with a repetition period of one week and chipping rate of 10.23 MHz and is the basis for precise position services (PPS). The C/A-code is a gold code sequence of length 1023 chips, with a repetition period of 1 ms, and a null to null bandwidth of about 2.046 MHz, ten times smaller that of the P-code [32]. C/A codes are intended for civil standard position services (SPS) and available for all users. The L_1 carrier is modulated by C/A code sequence combined with the navigation data inphase quadrature with the precision P-code combined with the data [36]. Thus, as shown in Fig. 3.3, the modulation of the civil C/A-code combined with the data is orthogonal to the modulation of the P-code added with the data on the L_1 signal. The navigation data consists of a low-rate (50 bits/sec) bit-stream describing the satellite orbits (ephemeris and almanac), clock corrections, and other parameters.

The received power levels on earth of the three GPS signals transmitted by the SVs are extremely weak and depend on the user elevation angle [32]. The minimum received signal power level, correspond at an elevation angle of $5°$ from the user's horizon are -160 dBW for the C/A-code, -163 dBW for P(Y)-code at L_1, and -166 dBW for P(Y)-code at L_2. Table 3.1 summarizes the GPS signal structure and the minimum received signal power at

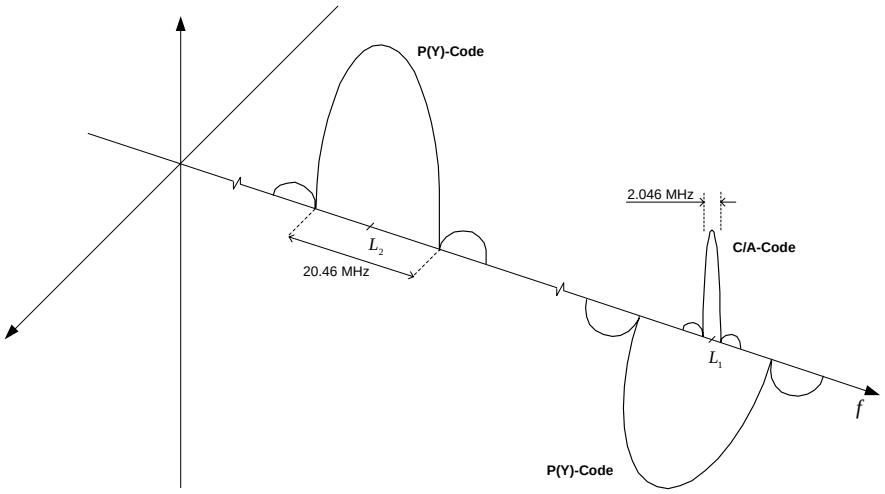

Fig. 3.3 GPS signal spectrum (positive side).

an elevation of $5°$. The change in the received power levels with respect to the user elevation angle and signal structure is illustrated in 3.4. GPS is limited by the weak penetration indoor of the satellite signal. Multipath effects are considered as one major sources of error in precise GPS positioning services. It affects the code range, the carrier phase measurements, and also the signal power which is an average of the composite of signal power of the direct and multipath components.

Table 3.1 GPS signal structure and minimum received signal power.

Signal	P(Y) & L_1	C/A & L_1	P(Y) & L_2
Carrier Frequency (MHz)	1575.42	1575.42	1227.60
PRN Codes (Mchips/sec)	10.23	1.023	10.23
Navigation Data (bits/sec)	50	50	50
Minimum Received Power (dBW)	-163	-160	-166

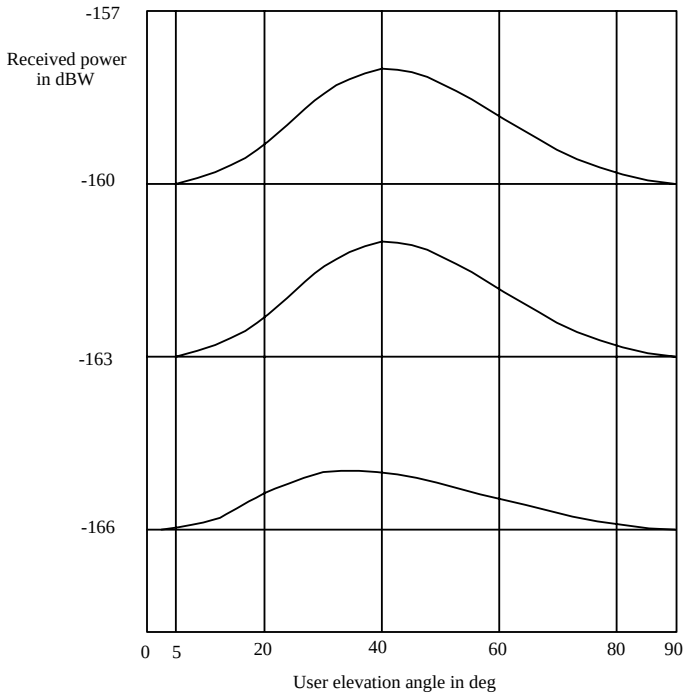

Fig. 3.4 User received minimum power levels with respect to the user elevation angle and signal structure.

3.4 MULTIPATH DELAY ESTIMATION TECHNIQUES

3.4.1 Channel Models

In a multipath fading environment, the channel can be modeled by a linear time-variant filter characterized by the complex-valued lowpass equivalent impulse response [26]

$$h(\tau, t) = \sum_{n=0}^{N} \alpha_n(t) e^{j\phi_n(t)} \delta(\tau - \tau_n(t)) \tag{3.1}$$

where N represents the number of propagation paths, $\alpha_n(t)$, $\phi_n(t)$ and $\tau_n(t)$ are the amplitude, the phase, and the propagation delay of n^{th} path, respectively. The channel is assumed to remain stationary during the considered observation time interval. In the sequel, the notation α_n, ϕ_n and τ_n will be adopted for simplicity.

By assuming that $h(\tau, t)$ is a zero mean, complex Gaussian random variable and wide-sense stationary, it can be described by the following fading autocorrelation function [16]

$$R_h(\tau, \Delta t) \stackrel{\triangle}{=} E[h^*(\tau; t)h(\tau; t + \Delta t)] \tag{3.2}$$

which gives a measure of the speed of channel variations. For $\Delta t = 0$, the autocorrelation reduces to $R_h(\tau, 0) \equiv R_h(\tau)$, called the intensity profile of the channel measuring the expected received power as a function of the delay τ. The delay-spread of the channel, denoted by T_m, is given by the region over which the $R_h(\tau)$ is not equal to zero and it indicates the degree of the time spreading in the channel. Thus, the reciprocal $B_c = 1/T_m$ is defined as the coherence bandwidth of the channel and it is a measure of the frequency selectivity. The multipath components have different path lengths resulting in different propagation delays. The delay spread of a channel depends in part on the proximity of scattering objects to the transmitter and receiver.

Due to the time variations in the medium structure, multipath delays are generally time-varying. The rate at which these-time delays vary, influences strongly the multipath channel effects on the signal. Time-variant multipath characteristics of the channel are analyzed using the spaced-time spaced-frequency correlation function of the channel given by [16]

$$R_H(\Delta f; \Delta t) \stackrel{\triangle}{=} E[H^*(f; t)H(f + \Delta f, t + \Delta t)]. \tag{3.3}$$

Here $H(f; t)$ is the Fourier transform of $h(\tau; t)$ and the time variations in the channel are measured by the time spacing parameter Δt.

Another way to express the rapidity of the channel variations and to reflect the Doppler effects, is by means of the Fourier transform of $R_H(\Delta f; \Delta t)$ with respect to the time spacing Δt as follows [26]

$$S_H(\Delta f; \nu) \stackrel{\triangle}{=} \int_{-\infty}^{+\infty} R_H(\Delta f; \Delta t)e^{-j\,2\pi\nu\,\Delta t} d\,\Delta t. \tag{3.4}$$

In particular for $\Delta f = 0$, the Doppler power spectrum of the channel is defined by

$$S(\nu) \equiv S_H(0, \nu) = \int_{-\infty}^{+\infty} R_H(\Delta t)e^{-j\,2\pi\nu\,\Delta t} d\,\Delta t. \tag{3.5}$$

The width of the region over which $S(\nu)$ is non-zero, is called the Doppler spread of the channel, denoted here by B_d, and its reciprocal is called the coherence time $(\Delta t)_c = 1/B_d$. The Doppler spread function characterizes the rapidity of the fading and is used in modeling Doppler shifts in the frequency domain caused by the relative motion of the transmitter, scatterers, and receiver. Slowly fading channel has a small Doppler spread B_d, which corresponds to a long coherence time.

Different types of fading channels do exist depending on the value of spread factor $T_m B_d$ of the channel, as well as, on the bandwidth $W = 1/T$ of the lowpass equivalent received signal [35]. For example, for a frequency nonselective flat and slowly fading channel, the spread factor is less than unity, $T_m B_d < 1$. In this case, the signal bandwidth is very small compared to the coherence bandwidth of the channel $W \ll B_c$, also the signalling interval is very small compared to the coherence time $T \ll (\Delta t)_c$ and the channel properties remains constant during a symbol interval. Similarly, if the spread factor is greater than unity $T_m B_d > 1$, it indicates that we have either a frequency selective channel $W > B_c$ or a fast fading channel $T > (\Delta t)_c$.

3.4.2 Conventional ML Based Approaches

After down-conversion of the received civil signal to baseband through mixing and filtering, the received GPS signal from one satellite in the presence of M-path channel can be modeled as [25], [37]

$$\begin{aligned} r(t) &= x(t) + n(t) \\ &= \sum_{i=0}^{M-1} a_i C(t-\tau_i) e^{j\theta_i} + n(t), \end{aligned} \tag{3.6}$$

where $C(t)$ is the real spread-spectrum code with a chipping rate $1/T_C$ much higher than the navigation data stream rate $1/T_D = 50$ bits/s, and $n(t)$ is an additive white Gaussian noise with power spectral density N_0. The time-variant a_i, τ_i and θ_i represent the attenuation factor, time delay, and phase for the i^{th} path, respectively. The estimation of the set of parameters $\{a_i, \tau_i, \theta_i\}$ is very essential for locating the line-of-sight path, and consequently for determining the GPS position, velocity and/or time.

Assuming that the down-converted signal $r(t)$ is completely defined in the observation time interval T_D, the conditional likelihood function based on the observation vector $\mathbf{r}$ for a given set of synchronization parameters $\mathbf{\Phi} = \{a, \tau, \theta\}$ is given by

$$p\big[\mathbf{r}\big|\mathbf{\Phi}\big] = \xi \exp\left\{ -\frac{1}{N_0} \int_{T_D} [r(t) - \hat{x}(t)]^2 dt \right\} \tag{3.7}$$

where ξ is just a positive constant independent of the synchronization parameters which can be neglected, and $\hat{x}(t)$ is the local trial signal replica generated at the receiver, modeling the estimated line-of-sight and multipath signals

$$\hat{x}(t) = \sum_{i=0}^{M-1} \hat{a}_i C(t-\hat{\tau}_i) e^{j\hat{\theta}_i}. \tag{3.8}$$

Multipath delay estimation techniques are based on the maximum likelihood theory [25] which are trying to estimate the set of parameters $\{\hat{a}, \hat{\tau}, \hat{\theta}\}$ by minimizing the mean squared error of the log-likelihood function (LLF) given by

$$L_{ML}(\hat{a}, \hat{\tau}, \hat{\theta}) = \mathrm{Re}\left\{ \int_{T_D} [r(t) - \hat{x}(t)]^2 dt \right\}. \tag{3.9}$$

Thus, the synchronization parameters are determined by differentiating the above LLF function with respect to the synchronization parameters, then setting the partial derivatives equal to zero. The partial derivative with respect to the time-delay estimate is given by [25]

$$\frac{\partial}{\partial \tau} L_{ML}(\hat{a}_i, \tau, \hat{\theta_i}) \bigg|_{\tau=\tau_i} = 2 \frac{\partial}{\partial \tau} \left[\mathrm{Re}\left\{ \left[R_{rc}(\tau) - \sum_{l=0, l\neq i}^{M-1} \hat{a}_l R_c(\tau - \hat{\tau}_l) e^{j\hat{\theta}_l} \right] e^{-j\hat{\theta}_i} \right\} \right]_{\tau=\tau_i}. \tag{3.10}$$

In the above equation, $R_{rc}(\tau)$ is the inphase/quadrature time-average cross-correlation function over the observation time interval T_D, given by

$$R_{rc}(\tau) = \frac{1}{T_D} \int_{T_D} r(t) C(t-\tau) dt, \tag{3.11}$$

and $R_c(\tau)$ is the reference time-average correlation function of the spreading code, given by

$$R_c(\tau) = \frac{1}{T_D} \int_{T_D} C(t)C(t-\tau)dt. \tag{3.12}$$

Different methods have been derived for finding the multipath delays, including coherent and non-coherent delay locked loops (DLLs) with proper early and late code spacings [34], [37] [38]. These methods are just trying to track the delay of the line-of-sight path by correlating the down-converted received signal with replicas of spreading codes locally generated by the DS-SS receiver.

Normally, by spreading the transmitted signal over a bandwidth larger than the coherence bandwidth of the channel, we can decrease the effects of multipath fading. The bandwidth spread makes it possible to separate different multipath signals if their relative delay difference exceeds one chip interval. Typically, distant reflectors have relatively large delay spread with more than one chip interval between successive paths, therefore, resulting multipaths can be removed by correlator-based mitigation techniques [25]. Thus, by maximizing the partial derivative equation of the LLF (3.9) with respect to the time-delay, the desired i^{th} path estimate can be written as follows,

$$\hat{\tau}_i = \arg\max_{\tau} \left[\mathrm{Re}\Big\{ \Big[R_{rc}(\tau) - \sum_{l=0, l\neq i}^{M-1} \hat{a}_l R_c(\tau - \hat{\tau}_l) e^{j\hat{\theta}_l} \Big] e^{-j\hat{\theta}_i} \Big\} \right]. \tag{3.13}$$

Similarly, by differentiating equation (3.9) with respect to the carrier phase and amplitude, and by solving the partial derivative equations for the M multipath components, the estimated carrier phase and amplitude for the i^{th} path are, respectively, given by [25]

$$\hat{\theta}_i = \arg\left[R_{rc}(\hat{\tau}_i) - \sum_{l=0, l\neq i}^{M-1} \hat{a}_l R_c(\hat{\tau}_i - \hat{\tau}_l) e^{j\hat{\theta}_l} \right] \tag{3.14}$$

$$\hat{a}_i = \mathrm{Re}\Big\{ \Big[R_{rc}(\hat{\tau}_i) - \sum_{l=0, l\neq i}^{M-1} \hat{a}_l R_c(\hat{\tau}_i - \hat{\tau}_l) e^{j\hat{\theta}_l} \Big] e^{-j\hat{\theta}_i} \Big\}. \tag{3.15}$$

Basic DLLs can estimate efficiently the multipath propagation delays if they are not overlapping and spaced at more $(1+\Delta)T_C$, where Δ being the loop discriminator value or early-late code spacing. However, the effects of offset paths are ignored. Several studies have been conducted to analyze the effects of multipath delays on coarse acquisition techniques [39] and fine acquisition techniques [40]. Delay locked loop (DLL) circuits generally fail to estimate closely-spaced multipaths with less than one chip interval, besides their convergence can be quite slow [25], [26], [37], [38]. Fig. 3.5 shows an example of S-curves obtained via a non-coherent DLL (NCDLL) with $SNR = 20$ dB for half chip and two chips spaced taps. We clearly notice that NCDLL fails to detect very closely spaced multipaths [35].

Another illustrative example in Fig. 3.6 shows the effect of multipath propagation on the S-curve with different early-late spacing values. Notice that the multipath components bias the tracking of the DLL. Smaller discriminator values may reduce this bias effect but are not able to eliminate it completely. However, as the excess path delays becomes smaller, they

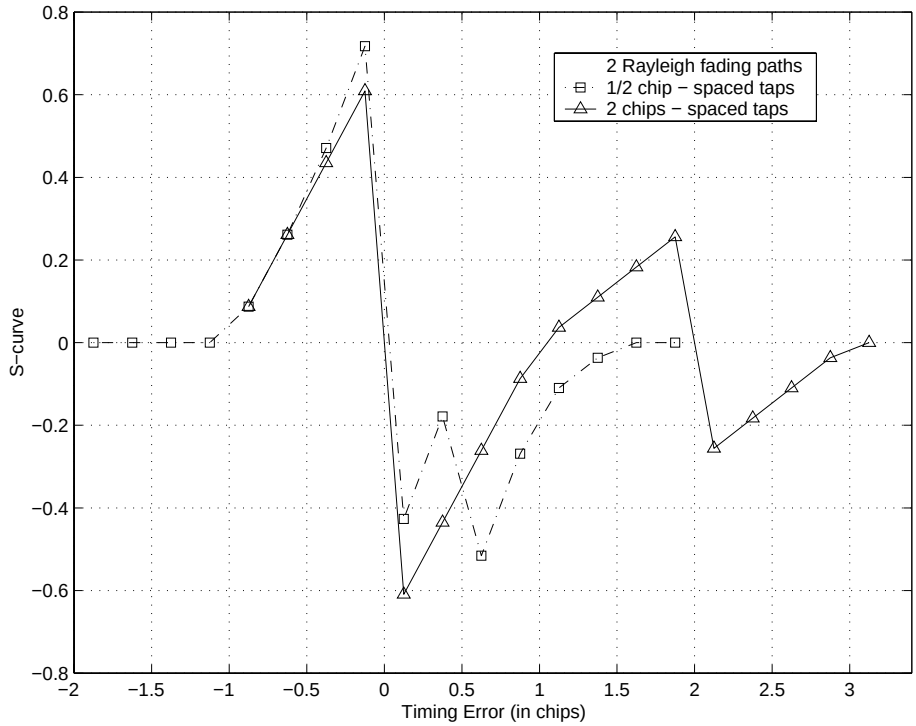

Fig. 3.5 Non-coherent DLL S-curve for a multipath channel.

result in shorter delays spread. Consequently, the LOS signal overlaps with the succeeding multipath components of short delays introducing significant error to the LOS path time and gain estimation.

Generally, multipath delay estimation techniques are based on the cross-correlation function (Eq. 3.11) of the down-converted signal de-spread with a copy of the spreading code locally generated by the DS-SS receiver. The advanced multipath estimating DLL techniques [38] are trying to approximate the overall cross-correlation using a set of reference correlation functions (Eq. 3.12) with certain delays, phases and amplitudes according to Eqs. (3.13), (3.14) and (3.15).

Many other techniques for mitigating the effects of multipath delays have been developed, including several subspace-based approaches. However, they are usually too complex for practical purposes and suitable only for systems employing short codes [41], [43], and the topic remains still an open area of research.

3.4.3 Multipath Delay Estimation Using Peak Tracking with Pulse Subtraction

Assuming that the locally generated code at the receiver side is locked to the received signal code (locally generated real code corresponds to the SV received signal code), by substituting equation (3.6) into (3.11), the cross-correlation function is simply expressed by

$$R_{rc}(\tau) = \frac{1}{T_D} \sum_{i=0}^{M-1} a_i e^{j\theta_i} \int_{T_D} C(t-\tau_i)C(t-\tau)dt + \frac{1}{T_D} \int_{T_D} n(t)C(t-\tau)dt. \quad (3.16)$$

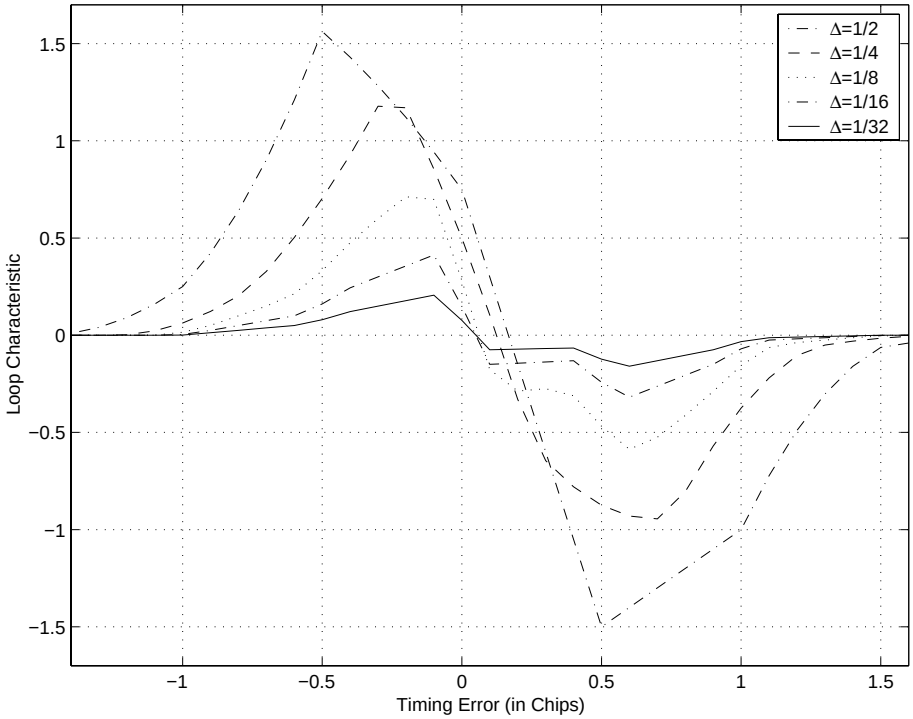

Fig. 3.6 Effect of multipath propagation on the S-curve of a non-coherent DLL using different discriminator values Δ and two paths channel.

Generally, practical GPS receivers perform averaging over short-time observation intervals less than the navigation data interval T_D to speed up the SV signals tracking. Normally, even-though we are considering averaging over a sufficiently large observation time interval, we shall consider the following biased estimator

$$R_{T_D^{'}}(\tau) = \begin{cases} \frac{1}{T_D^{'}} \int_{T_D^{'}} C(t)C(t-\tau)dt & \text{for } |\tau| < T_D^{'} \\ 0 & \text{otherwise} \end{cases}$$

whose expected value or mean is given by [42]

$$E\{R_{T_D^{'}}\} = R(\tau)\left(1 - \frac{|\tau|}{T_D^{'}}\right) = R(\tau) \triangle (\tau, T_D^{'}). \tag{3.17}$$

Here, $\triangle(\tau, T_D^{'})$ denotes a triangular function defined as follows

$$\triangle(\tau, T_D^{'}) = \begin{cases} 1 - |\tau|/T_D^{'} & |\tau| \leq T_D^{'} \\ 0 & \text{otherwise}. \end{cases} \tag{3.18}$$

Recalling the Gaussian nature of the random process as well as the mean of the biased estimator (3.17), the expectation of the above cross-correlation function (3.16) becomes

$$\begin{aligned} E\{R_{rc}(\tau)\} &= \sum_{i=0}^{M-1} a_i e^{j\theta_i} R_c(\tau - \tau_i)\left(1 - \frac{|\tau - \tau_i|}{T_D^{'}}\right) \\ &= \sum_{i=0}^{M-1} a_i e^{j\theta_i} R_c(\tau - \tau_i) \triangle (\tau - \tau_i, T_D^{'}). \end{aligned} \tag{3.19}$$

Notice that the expected value of the cross-correlation function is expressed simply as a weighted sum of delayed correlation functions times triangular windows with certain amplitude and phase specific to each signal path. The correlation effectively amplifies the underlying BPSK data signal, with an amplification factor equal to the length of the PRN Gold code sequence.

The proposed peak tracking with pulse subtraction approach for estimating the multipath delays is analogous to the advanced DLL techniques [25] in the sense that it is trying to estimate the overall cross-correlation function using a set of reference functions, but with different and simpler implementation. This approach is based on the search of the global maxima of the cross-correlation function (Eq. 3.16). Then, the contribution of each selected maximum is reduced from the overall cross-correlation using the autocorrelation function of a rectangular pulse [54]. The proposed technique is described further by the following algorithm:

- find the global maximum
  $\hat{\tau}_1 = \arg\max_\tau \left[|R_{rc}(\tau)|\right].$
- compute the residual cross-correlation function
  $R_{rc,1}(\tau) = \left|R_{rc}(\tau) - R_{rc}(\hat{\tau_1}) \triangle (\tau - \hat{\tau_1})\right|.$
- find the global maximum of the residual cross-correlation function
  $\hat{\tau}_2 = \arg\max_\tau \left[|R_{rc,1}(\tau)|\right].$
- estimate successively the next $M_{est} - 1$ maxima
  $\hat{\tau}_k = \arg\max_\tau \left[\left|R_{rc}(\tau) - \sum_{l=1}^{k-1} R_{rc,l}(\hat{\tau}_l) \triangle (\tau - \hat{\tau}_l, T_C)\right|\right], \;\; k = 2, 3, \ldots, M_{est}.$

Here $R_{rc,l}(\tau)$ is the residual cross-correlation function after l^{th} peak subtraction, M_{est} is an estimate for the number of multipaths of the channel (it can be taken equal to the number of fingers (or correlators) as in a Rake receiver). By using the ideal code correlation pulse for subtracting the contribution of each channel path, we are able to detect very closely-spaced multipaths within less than one chip period ($|\tau_l - \tau_k| < T_C$) [54].

Only a simplified generic structure is presented above to describe the algorithm. However, instead of choosing the global maximum of the envelope of the residual correlation function as a true multipath component, we can take into account the merging phenomena. Hence, we try a set of multipath delays within a certain window around the global maxima with different weights, and the final estimates are those which give the best approximation of the correlation function in the mean square error sense.

3.4.4 Multipath Delay Estimation Based on Teager-Kaiser Operator

In this section, we introduce an innovative multipath delay estimation approach based on the nonlinear quadratic Teager-Kaiser operator that exploit the structure of the cross-correlation function (Eq. 3.11) for estimating sub-chip spaced multipath components.

The nonlinear quadratic TK operator was first introduced for measuring the real physical energy of a system [44], [45]. The energy of a generating system of a simple oscillation

signal was computed as the product of the square of the amplitude and the frequency of the signal. It was found that this nonlinear operator exhibits several attractive features such as simplicity, efficiency and ability to track instantaneously-varying spatial modulation patterns. Since its introduction, several applications have been derived for one-dimensional signal processing [S3], [46] (note that proposition 3 in [46] is erroneous as pointed in [47]) and two-dimensional signal processing [48], [55].

The continuous-time TK energy operator of a complex-valued signal $x(t)$ is defined as follows [S3]

$$\Psi_c[x(t)] = \dot{x}(t)\dot{x}^*(t) - \frac{1}{2}[\ddot{x}(t)x^*(t) + x(t)\ddot{x}^*(t)]. \tag{3.20}$$

Similarly, the discrete-time Teager operator of a complex valued signal is given by

$$\Psi_d[x(n)] = x(n-1)x^*(n-1) - \frac{1}{2}[x(n-2)x^*(n) + x(n)x^*(n-2)]. \tag{3.21}$$

Many useful properties of this nonlinear quadratic operator have been derived, and the analogy with the discrete-time domain has also been established [49], [56].

We notice that applying the continuous-time TK operator to the ideal reference correlation function of the spreading code which is characterized by the triangular shape (Eq. 3.18), we obtain

$$\Psi_c[\triangle(t, T_C)] = \frac{\Pi(t, T_C)}{T_C^2} + \frac{\triangle(t, T_C)\delta(t)}{T_C}, \tag{3.22}$$

where $\delta(t)$ is the Dirac function, and $\Pi(t, T_C)$ stands for a rectangular function with unit amplitude and duration $2T_C$ centered at $t = 0$ defined as

$$\Pi(t, T_C) \triangleq \begin{cases} 1 & |t| \leq T_C \\ 0 & \text{otherwise.} \end{cases}$$

Obviously, Eq. (3.22) shows that the TK operator applied to a triangular function provides a clear time-aligned peak location of the triangular pulse in the presence of a certain 'noise' floor.

Assuming now that the cross-correlation function is the sum of M triangular pulses as follows

$$R(t) = \sum_{i=0}^{M} a_i \triangle (t - t_i, T_C) e^{j\theta_i}, \tag{3.23}$$

where a_i, t_i and θ_i denote the amplitude, delay and phase, respectively. By applying the TK operator to the above equation we obtain

$$\begin{aligned} \Psi_c[R(t)] \;=\; & \frac{1}{T_C^2}\left[\left(\sum_{i=0}^{M} a_i \text{sign}(t - t_i)\Pi(t - t_i, T_C)\cos\theta_i\right)^2\right. \\ & \left. + \left(\sum_{i=0}^{M} a_i \text{sign}(t - t_i)\Pi(t - t_i, T_C)\sin\theta_i\right)^2\right] \\ & + \frac{1}{2T_C}\left[R^*(t)\left(\sum_{i=0}^{M} a_i\delta(t - t_i)e^{j\theta_i}\right) + R(t)\left(\sum_{i=0}^{M} a_i\delta(t - t_i)e^{-j\theta_i}\right)\right]. \end{aligned} \tag{3.24}$$

Notice that the above expression becomes very large if the time variable t is equal to one of the true delays t_i. Thus, equation (3.24) shows that the TK operator is capable of tracking very accurately the peak locations of the triangular pulses within certain 'noise' floor [57] independently of the delay spacing between the multipaths.

By exploiting the above properties of the quadratic operator, we found out that by applying this nonlinear TK operator to the specific cross-correlation function (Eq. 3.11) of a GPS receiver, one can easily estimate the multipath delays introduced by the channel. The multipath delays are simply estimated by selecting the time location of the highest (strongest) peaks of the Teager-Kaiser operator output function (equal to the number of fingers in the Rake receiver). Simulation results provided in publications [P6]-[P8] show the high performance of this innovative technique.

Chapter 4

Summary of Publications

4.1 RECEIVER SYNCHRONIZATION STUDIES

A general approach for discrete-time modeling and simulation of continuous-time signals and systems based on digital interpolation techniques is introduced in [P1]. We demonstrate that polynomial interpolation utilizing the generalized Farrow structure results in efficient polynomial signal processing models with moderate computational complexity. Normally, the lowest sampling rates which are sufficient for system modeling, are not sufficient for obtaining informative and accurate models. In cases where computational efficiency is an issue, different sampling rates can be used in different blocks to reduce the computational burden. In cases where there is a need to locate, e.g., the local maxima, minima, or zero crossings of a signal, higher order oversampling rate is needed. It is common practice also to use oversampling factors which are an order of magnitude higher than what is required from the sampling theory point of view.

The generalized Farrow structure allows, with low additional computational complexity, to compute several new samples at arbitrary points between the existing samples. Thus, it is very easy to get the signal sample values in a flexible way in what ever time instances they are needed. Furthermore, it is possible also to implement iterative procedures for estimating accurately, e.g., the maximum value of a continuous-time signal as well as the location of the maximum. In [P1] we also develop simple modifications of the Farrow structure which result in efficient polynomial-based differentiators for approximating the continuous-time derivative of a signal from its discrete-time samples. The Farrow structure discussed in [P1] is the basis of the proposed ML-based synchronization algorithms. As another potential application and a topic for future studies, Farrow-based derivative approximations could be utilized for efficiently calculating the continuous-time Teager function of a discrete-time signal. This could lead to efficient implementation structures for the Teager-based delay estimation techniques.

In [P2], a polynomial-based maximum likelihood technique for jointly estimating the symbol timing and carrier phase of digital receivers for the data-aided case is established. This technique is based on low order polynomial approximation of the log-likelihood func-

tion by using the Farrow structure. An extension of the proposed polynomial-based ML technique to the non-data-aided systems is derived in [P3]. Different simulations using the Lagrange and optimized interpolator are performed for both DA and NDA systems and compared with the theoretical case. The results show the high performance of the optimized interpolator compared to the Lagrange interpolator especially if we want to make use of shorter block lengths to obtain fast acquisition. However, the NDA approach requires more computation than the DA approach for estimating the polynomial-based likelihood function. Also, NDA based phase estimation is feasible only in case of PSK modulations.

In [P4], the effect of the frequency offset or Doppler shift on the performance of the digital receiver is analyzed while adjusting the symbol timing and the carrier phase. We demonstrated that the proposed synchronization scheme performs quite well within a relatively small range of frequency offset values with respect to the symbol period. Under the same assumption that the frequency offset is much smaller than the symbol period, symbol timing and carrier phase recovery can be done prior to the frequency error correction. Thus, we introduced in [P5] a frequency estimator that is directly derived from the carrier phase estimate. The proposed estimator is simple to implement and is particularly suited for this type of digital receiver architectures. Also, it performs fairly well when compared with the Fitz [50] and the Luise-Reggiannini [15] frequency estimators, in the presence of substantial carrier frequency offset.

4.2 MULTIPATH DELAY ESTIMATION STUDIES

Correlation estimation properties related to DS-CDMA receivers have been studied in [P6]. We showed the influence of the coherent integration and the non-coherent averaging length on multipath delay estimation, and the importance of the considered observation time interval length. In [P7], we introduced two techniques with subchip resolution capability for estimating closely-spaced overlapped multipath components suited for GSP system as well as for other spread spectrum CDMA systems. The first innovative technique is very simple and quite efficient based on Teager-Kaiser operator. It exploits the properties of the cross-correlation function between the received signal and the reference despreading code replica generated at the receiver in order to estimate accurately overlapped multipath delays independently of the delay spacing between the multipaths. The second algorithm is based on peak tracking with pulse subtraction which approximates the input correlation function using the superposition of a set of reference correlation pulses. Simulation results of a GPS receiver using different Rayleigh fading channels show the good performance of the proposed techniques. Also the obtained results are considered to be remarkable considering the computation complexity of these approaches in comparison to the advanced maximum likelihood based DLL techniques. Extension of the proposed algorithms to the case of asynchronous multiuser WCDMA systems is presented in [P8]. Simulation results in the presence of multiple interfering users and Rayleigh fading multipath channels are presented. It is demonstrated that the Teager-Kaiser technique is near far-resistant, and its performance in the presence of closely spaced multipaths is much better compared to the peak tracking with subtraction method.

The problem of resolving closely-spaced overlapped multipath components can be considered new, and has recently raised up the interest after its strong influence on the high

precision accuracy of geolocation solutions. Few good research articles exist in the literature dealing with this problem, they generally treat the case of only two paths that are present, and not very practical for implementation [37], [43], [51], [52].

4.3 AUTHOR'S CONTRIBUTION TO THE PUBLICATIONS

The research work of this thesis was carried out at the Institute of Communications Engineering (formerly Telecommunications Laboratory), Tampere University of Technology as one partner in the projects "Advanced Transceiver Architectures and Implementations for Wireless Communications" and "Analog and Digital Signal Processing Techniques for Highly Integrated Transceivers". The author has been a member of an active research group involved in studying and developing DSP algorithms for highly integrated digital receivers, as well in building COSSAP and Matlab simulation models. The members of the research group have been in close collaboration with the author and the whole project has been supported and guided by the thesis supervisor Prof. Renfors. However, the author's contribution to all of the publications has been essential in that he developed the theoretical framework, prepared the manuscript, and performed the experiments.

This thesis includes eight publications [P1]-[P8]. They are categorized under two main topics: estimation of the synchronization parameters for digital receivers with non-synchronized sampling clock [P1]-[P5], and estimation of closely-spaced multipath delays in CDMA systems [P6]-[P8]. In particular, the author's main contributions to these publications are as follows. In [P1], the author formulated and simulated the general approach for discrete-time modeling of continuous-time signals and systems based on the generalized interpolation technique which is efficiently implemented using minor modifications to the Farrow structure. Originally, the author introduced the concept of derivative approximation and the preliminary idea for integration using simple modifications of the Farrow structure. In [P2] and [P3], the author derived the likelihood functions for systematic synchronization schemes, made the extension for jointly estimating the symbol timing and carrier phase for both DA and NDA systems, and carried out the simulations. In [P4] and [P5], the author studied and simulated the effect of frequency offset on the synchronization scheme, and derived a new frequency estimator suitable for the proposed digital receiver type. Optimization of the Farrow structure based filters, needed in [P1]-[P5], are performed by Dr. Vesma.

In [P6] and [P7], the author is the founder of the multipath delay estimation techniques based on Teager-Kaiser operator. The idea of pulse subtraction technique was originally proposed by Prof. Renfors. The author derived and simulated the algorithms. In [P8], these algorithms have been applied and tested in the WCDMA multiuser environment using existing COSSAP simulation model. The author conducted experimental studies and wrote the manuscript.

Chapter 5

Conclusions

Currently, the main driving force behind the software radio development is the coexistence of several radio communication systems as a result of the high competition between Americans, Asians, and Europeans. The ultimate goal of designing a single-chip, flexible wireless transceiver supporting multimode and multistandard compatibility introduced new challenges in receiver architecture designs. The current trend is to push the analog/digital interface towards the antenna to simplify the analog parts and allow the implementation of most receiver functions digitally, increasing therefore the flexibility, configurability, and integrability. In fact, existing communication standards are using different data rates, and consequently they employ different master clock rates. By using a digital receiver architecture with a free running clock oscillator, receiver complexity can be substantially reduced by employing only a single master clock, and the other needed clock rates can be generated virtually by means of sampling rate conversion. As one important functionality, these new receivers require flexible and efficient synchronization algorithms which depend on the system requirements and receiver architecture design.

The first part of this research work introduces new maximum likelihood based symbol timing and carrier phase estimators suitable for digital receivers with non-synchronized sampling clock. Polynomial approximations of the likelihood functions using the Farrow-based interpolation technique were established for both DA and NDA forms. The simulations demonstrate the efficiency and excellent performance of the block-based feedforward estimators. The proposed approach provides an efficient and practical way for approximating very closely the ideal maximum likelihood estimate, especially for the DA case. The Farrow structure we are considering is particularly suitable for digital implementation.

However, the NDA case requires more computational burden because the averaging of the likelihood function can not be done in the polynomial coefficient domain as for the DA case. Therefore, further studies with respect to the computational complexity of the NDA technique are needed for practical applications.

Another essential receiver functionality closely related to synchronization is propagation delay estimation which is the basis for geolocation positioning solutions. The rapid evolution of digital communication systems and the new requirements imposed by the standardization authorities brought various consumer electronics device types and a high demand on

new communication services, such as mobile phone positioning with high and reliable accuracy. Even if safety was the primary motivation for mobile positioning, a lot of commercial applications have already emerged in the market.

However, multipath effects of the mobile channel could degrade the location estimate substantially, specially in the case of shorter excess path delays which result in overlapped fading multipath components that introduce significant errors to the LOS path time and gain estimation. Estimation of closely-spaced multipath components is regarded as a killer issue in location estimation, considered as one of the major sources of errors in high precision geolocation solutions, and still it is an open topic for research work.

In the second part of this thesis work, we introduced innovative techniques with sub-chip resolution capability for multipath delay estimation based on peak tracking with pulse subtraction and Teager-Kaiser quadratic operator both suited for spread spectrum CDMA systems, and we focused our study to the case of GPS receivers. Simulations results confirmed the high performance of Teager-based technique compared to the peak tracking with pulse subtraction method for all cases of closely-spaced multipaths within less than half chip period. The ability of solving closely-spaced paths in the presence of overlapped multipath components comes from the exploitation of the properties of the cross-correlation function. This new techniques are extremely simple and very efficient for estimating closely-spaced multipaths with much less computational complexity compared, e.g., to the conventional delay-locked loops and subspace-based multipath delay estimation methods [25], [41].

In general, for each shape of the reference correlation function or pulse shaping filter used, there may exist a linear or nonlinear operator capable of estimating easily the multipath delays. It remains as a challenging topic for future work is to generalize the Teager-based technique, and to derive other linear or nonlinear operators capable of tracking multipath delays in different communication systems.

References

[1] FCC docket No. 94–102, Fourth memorandum opinion and order, September 8^th, 2000.

[2] J. Syrjärinne, *Studies of modern techniques for personal positioning.* PhD Thesis, Tampere University of Technology, 2001.

[3] Benefon Oyj., "Personal navigation phone GSM + GPS," http://www.benefon.com.

[4] Cellpoint Inc., "Mobile location system," http://www.cellpoint.com/pdf/MLS.pdf.

[5] G. Christensen, "Location based services," http://www.mobilein.com.

[6] R. Baines, "The DSP bottleneck," *IEEE Communications Magazine*, vol. 33, pp. 46–54, May 1995.

[7] R.J. Lackey and D.W. Upmal, "Speakeasy: the military software radio," *IEEE Communications Magazine*, vol. 33, pp. 56–68, May 1995.

[8] J. Mitola, "The software radio architecture," *IEEE Communications Magazine*, vol. 33, pp. 24–38, May 1995.

[9] M. Laddomada, F. Daneshgaran, M. Mondin and R.M. Hickling, "A PC-based software receiver using a novel front-end technology," *IEEE Communications Magazine*, vol. 39, pp. 136–145, August 2001.

[10] T. Hentshel and G. Fettweis, "Sample rate conversion for software radio," *IEE Communications Magazine*, August, 2000, pp. 142–150.

[11] Harris Corporation, "RF communications," *Annual Report* 2001, http://www.harris.com/harris/ar/01/rfcomm.html.

[12] H. Meyr and G. Ascheid, *Synchronization in digital communications, phase, frequency locked loops, and amplitude control*. Wiley Sons, 1989.

[13] F. M. Gardner, "Interpolation in digital modems - Part I: fundamentals," *IEEE Trans. Commun.*, vol. 41, pp. 501–507, March 1993.

[14] L. Erup, F. M. Gardner, and R. A. Harris, "Interpolation in digital modems - Part II: implementation and performance," *IEEE Trans. Commun.,* vol. 41, pp. 998–1008, June 1993.

[15] U. Mengali and A. N. D'Andrea, *Synchronization techniques for digital receivers.* Plenum Press, 1997.

[16] J. G. Proakis, *Digital communication.* McGraw-Hill, 1989.

[17] C. W. Farrow, "A continuously variable digital delay element," in *Proc. IEEE Int. Symp. Circuits & Syst.*, Espoo, Finland, June 1988, pp. 2641–2645.

[18] L.P. Sabel and W.G. Cowley, "Block processing feedforward symbol timing estimator for digital modems," *Electronics Letters,* vol. 30, pp. 1273–1274, August 1994.

[19] W.G. Cowley and L.P. Sabel, "The performance of two symbol timing recovery algorithms for PSK demodulators," *IEEE Transactions on Communications,*, vol. 42, pp. 2345–2355, June 1994.

[20] H. Meyr, M. Moeneclaey, and S. A. Fechtel, *Digital communication receivers: synchronization, channel estimation and signal processing.* John Wiley & Sons, 1998.

[21] F. M. Gardner, "Demodulator reference recovery techniques suited for digital implementation," *ESA Final Report,* Aug. 1988.

[22] J. Vesma, *Optimization and applications of polynomial-based interpolation filters.* Ph.D. Thesis, Tampere University of Technology, Tampere, Finland, May 1999.

[23] T.I Laakso, V. Välimäki, M. Karjalainen, and U.K. Laine, "Splitting the unit delay," *IEEE Signal Processing Magazine.* vol. 13, pp. 30–60, January 1996.

[24] J. Vesma and T. Saramäki, "Interpolation filters with arbitrary frequency response for all-digital receivers," *Proc. IEEE Int. Symp. Circuits & Syst.*, Atlanta, GA, May 1996, pp. 568–571.

[25] R.Van Nee, *Multipath and multi-transmitter interference in spread-spectrum communication and navigation system*. Delft University Press, 1995.

[26] M.K. Simon and M.S. Alouini, *Digital communication over fading channels; a unified approach to performance analysis*. John Wiley & Sons, Inc., 2000.

[27] 3^{rd} Generation Partnership Project, *Technical Report* 25.827, 2001-03, http://www.3gpp.org.

[28] K. Kalliojärvi, "Terminal positioning in WCDMA," *in Proc. EUSIPCO 2000,* Tampere, Finland, September 2000, pp. 2269–2272.

[29] T.S. Rappaport, J.H. Reed and B.D. Woerner, "Position location using wireless communications on highways of the future," *IEE Communications Magazine,* October, 1996, pp. 33–41.

[30] L. Lopes, E. Villier and B. Ludden, "GSM standards activity on location," *IEE Colloquium on Novel Methods of Location and Tracking of Cellular Mobiles and Their System Applications,* 1999, pp. 1–7.

[31] M. D. Goran and R. E. Richton, "Geolocation and assisted GPS," *IEEE Communications Magazine,* Feb. 2001, pp. 123–125.

[32] E.D. Kaplan, *Understanding GPS; principles and applications.* Artech House Inc., 1996.

[33] P. Enge and Pratap Mistra, "Scanning the issue/technology; special issue on GPS," *Proc. of the IEEE,* vol. 87, No. 1, January 1999, pp. 3–15.

[34] M. Braasch and A.J.V. Dierendonck, "GPS receiver architectures and measurements," *Proc. of the IEEE,* vol. 87, No. 1, January 1999, pp. 48–64.

[35] J.S. Lee and L.E. Miller, *CDMA systems engineering handbook.* Artech House, 1998.

[36] http://www.colorado.edu/geography/gcraft/notes/gps/

[37] M.C. Laxton and S.L. DeVilbis, "GPS multipath mitigation during code tracking," *in Proc. of the American Control Conference*, Albuquerque, New Mexico, pp. 1429–1433, June 1997.

[38] R. Van Nee, J. Siereveld, P. Fenton, and B. Townsend, "The multipath estimating delay lock loop: approaching theoretical accuracy limits," *in Proc. of IEEE Position, Location, and Navigation Symposium,* April 1994, pp. 246–251.

[39] B. Ibrahim and A. Aghvami, "Direct sequence spread spectrum matched filter acquisition in frequency-selective Rayleigh fading channels," *IEEE Journal on Selected Areas in Communications,* vol. 12, pp. 885–890, June 1994.

[40] W. Sheen and G.L. Stüber, "Effects of multipath fading on delay-locked loops for spread spectrum systems," *IEEE Trans. on Communications,* vol. 42, pp. 1947–1956, February/March/April 1994.

[41] P. Luukkanen, and J. Joutsensalo, "Comparison of MUSIC and matched filter delay estimators in DS-CDMA," *in Proc. of IEEE Personal, Indoor and Mobile Radio Communications*, vol. 3, 1997, pp. 830–834.

[42] A. Papoulis, *Signal analysis*. McGraw-Hill, 1988.

[43] Z. Kostić, G. Pavlović, "Resolving sub-chip spaced multipath components in CDMA communication systems," *in Proc. of IEEE VTC*, vol. 1, 1993, pp. 469–472.

[44] J. F. Kaiser, "On a simple algorithm to calculate the 'energy' of a signal," *Proc. IEEE ICASSP–90*, Albuquerque, New Mexico, pp. 381–384, April 1990.

[45] J. F. Kaiser, "On Teager's energy algorithm and its generalization to continuous signals," *Proc. 4th IEEE Digital Signal Processing Workshop*, Mohonk (New Paltz), NY, September 1990.

[46] P. Maragos, J. F. Kaiser, and T. F. Quatieri, "Energy separation in signal modulations with application to speech analysis," *IEEE Trans. Signal Processing*, vol. 41, no. 10, pp. 3024–3051, October 1993.

[47] V.P. Stokes and P. Händel, "Comments on "On amplitude and frequency demodulation using energy operators," *IEEE Transactions on Signal Processing*, vol. 46, no. 2, pp. 506–507, February 1998.

[48] J. Fang and L. Atlas, "Quadratic detectors for energy estimation," *IEEE Transactions on Signal Processing*, vol. 43, no. 11, pp. 2582–2594, November 1995.

[49] J. F. Kaiser, "Some useful properties of Teager's energy operators," *Proc. IEEE ICASSP–93*, vol. III, pp. 149–152, April 27–30, 1993.

[50] M.P. Fitz, "Further results in the fast estimation of a single frequency," *IEEE Trans. Commun.*, Vol. 42, pp. 862–864, March 1994.

[51] J. Soubielle and I. Fijalkow, "GPS positioning in a multipath environment," *IEEE Transactions on Signal Processing*, vol. 50, no. 1, pp. 141–150, January 2002.

[52] G. Fock, J. Baltersee, P. Schulz-Rittich and H. Meyr, "Channel tracking for Rake receivers in closely spaced multipath environment," *IEEE Journal on selected areas in communications*, vol. 19, no. 12, pp. 2420–2431, December 2001.

[53] R. Hamila, M. Renfors, G. Gunnarsson, M. Alanen, "Data processing for mobile phone positioning," *in Proc. VTC'99*, Amsterdam, Netherlands, Sept. 1999, pp. 446–449.

[54] R. Hamila, S. Lohan and M. Renfors, "Multipath delay estimation in GPS receivers," *In Proc. Nordic Signal Processing Symposium (Norsig'2000)*, Kolmården, Sweden, pp. 417–420, June 2000.

[55] F. Alaya Cheikh, R. Hamila, M. Gabbouj and J. Astola, "Impulse noise removal in highly corrupted color images," *Proc. 1996 IEEE International Conference on Image Processing*, ICIP-96, Vol.1, pp. 997–1000, Lausanne, Switzerland, 1996.

[56] R. Hamila, "Teager energy operator; theory and Applications," *Licentiate Thesis*, Tampere University of Technology, December 1998.

[57] R. Hamila and M. Renfors, "Nonlinear operator for multipath channel estimation in GPS receivers," *In The 7th IEEE International Conference On Electronics, Circuits & Systems*, Jounieh, Lebanon, pp. 352–356, December 2000.

Publications

Publication 1

R. Hamila, J. Vesma, T. Saramäki and M. Renfors, "Discrete-Time Simulation of Continuous-Time Systems Using Generalized Interpolation Techniques," *in Proc. 1997 the Summer Computer Simulation Conference*, SCSC'97, Arlington, Virginia, USA, July 1997, pp. 914–919.

Publication 2

R. Hamila, J. Vesma, H. Vuolle, and M. Renfors, "Joint Estimation of Carrier Phase and Symbol Timing Using Polynomial-Based Maximum Likelihood Technique," *in the IEEE 1998 International Conference on Universal Personal Communications,* ICUPC'98, Florence, Italy, October 1998, pp. 369–373.

Publication 3

R. Hamila, J. Vesma, H. Vuolle, and M. Renfors, "NDA Maximum Likelihood Approach for Timing and Phase Adjustment by Polynomial-Based Interpolation," *in Proc. 6th IEEE International Workshop on Intelligent Signal Processing and Communication Systems,* ISPACS'98, Melbourne, Australia, Nov. 1998, pp. 248–252.

Publication 4

R. Hamila, J. Vesma, H. Vuolle, and M. Renfors, "Effect of Frequency Offset on Carrier Phase and Symbol Timing Recovery in Digital Receivers," *in Proc. 1998 URSI International Symposium on Signals, Systems, and Electronics*, ISSSE'98, Pisa, Italy, September 1998, pp. 247–252.

Publication 5

R. Hamila, M. Renfors, "New Maximum Likelihood Based Frequency Estimator for Digital Receivers," *in Proc. IEEE Wireless Communications and Networking Conference*, WCNC´99, New Orleans, USA, Sept. 1999, pp. 206–210.

Publication 6

R. Hamila, S. Lohan, and M. Renfors, "Effect of Correlation Estimation on Multipath Delay Estimation Techniques in DS-CDMA Systems," *in Proc. of 4th International Symposium on Wireless Personal Multimedia Communications*, WPMC'01, Aalborg, Denmark, September 2001, pp. 331–335.

Publication 7

R. Hamila, S. Lohan, and M. Renfors, "Novel Technique for Closely-Spaced Multipath Delay Estimation in DS-CDMA Systems," *Submitted to Signal Processing*, (EURASIP).

Publication 8

S. Lohan, R. Hamila, and M. Renfors, "Performance Analysis of an Efficient Multipath Delay Estimation Approach in a CDMA Multiuser Environment," *in Proc. of 12th IEEE International Symposium on Personal, Indoor and Mobile Radio Communications,* PIMRC´01, San Diego, California, USA, Sept. 2001, pp. 6–10.

Tampereen teknillinen korkeakoulu
PL 527
33101 Tampere

Tampere University of Technology
P. O. B. 527
FIN-33101 Tampere Finland